

Sec17/Sec18 can support membrane fusion without help from completion of SNARE zippering

Hongki Song^{1†}, Thomas L Torng^{1†}, Amy S Orr¹, Axel T Brunger², William T Wickner^{1*}

¹Department of Biochemistry and Cell Biology Geisel School of Medicine at Dartmouth, Hanover, United States; ²Howard Hughes Medical Institute and Department of Molecular and Cellular Physiology Stanford University, Stanford, United States

Abstract Membrane fusion requires R-, Qa-, Qb-, and Qc-family SNAREs that zipper into RQaQbQc coiled coils, driven by the sequestration of apolar amino acids. Zippering has been thought to provide all the force driving fusion. Sec17/ α SNAP can form an oligomeric assembly with SNAREs with the Sec17 C-terminus bound to Sec18/NSF, the central region bound to SNAREs, and a crucial apolar loop near the N-terminus poised to insert into membranes. We now report that Sec17 and Sec18 can drive robust fusion without requiring zippering completion. Zippering-driven fusion is blocked by deleting the C-terminal quarter of any Q-SNARE domain or by replacing the apolar amino acids of the Qa-SNARE that face the center of the 4-SNARE coiled coils with polar residues. These blocks, singly or combined, are bypassed by Sec17 and Sec18, and SNARE-dependent fusion is restored without help from completing zippering.

***For correspondence:**

William.T.Wickner@dartmouth.edu

[†]HS and TL are co-first authors of this work

Competing interest: See page 22

Funding: See page 22

Received: 16 February 2021

Accepted: 30 April 2021

Published: 04 May 2021

Reviewing editor: Josep Rizo, University of Texas Southwestern Medical Center, United States

© Copyright Song et al. This article is distributed under the terms of the [Creative Commons Attribution License](https://creativecommons.org/licenses/by/4.0/), which permits unrestricted use and redistribution provided that the original author and source are credited.

Introduction

Membrane fusion requires Rab-family GTPases and SNARE proteins. SNAREs constitute four families, termed R, Qa, Qb, and Qc (*Fasshauer et al., 1998*). Each of them has an N-domain, an α -helical SNARE domain of 50–60 aminoacyl residues with heptad-repeat apolar residues, and often a C-terminal membrane anchor. Each SNARE α -helical turn is termed a 'layer.' The central '0-layer' of each fully-assembled SNARE complex has inwardly-oriented arginyl (for R-SNAREs) or glutaminyl (for Qa, Qb, and Qc SNAREs) residues, forming a polar center to the otherwise hydrophobic core of the 4-helical SNARE bundle (*Sutton et al., 1998*). The SNARE domain layers are numbered from the 0-layer, in the positive direction toward the SNARE C-termini and in the negative direction toward the N-domains. Prior to 4-SNARE assembly, individual SNARE domains are random coil (*Fasshauer et al., 1997; Hazzard et al., 1999*). Sec1/Munc18 (SM) family proteins catalyze the N- to C-directional assembly of SNAREs anchored to each tethered membrane (*Fiebig et al., 1999; Sørensen et al., 2006; Baker et al., 2015; Orr et al., 2017; Jiao et al., 2018*). Each SNARE domain transitions from random coil to α -helix as the heptad-repeat apolar amino acyl residues become sequestered into the interior of the coiled coils (*Fasshauer et al., 1997; Sutton et al., 1998*). This hydrophobic collapse relies on the exclusion of water and is the driving force for SNARE assembly (*Sørensen et al., 2006*). Completion of SNARE zippering can release up to 40 kBT per SNARE complex (*Gao et al., 2012; Min et al., 2013; Zhang, 2017*) to overcome the 40–90 kBT hydration barrier for membrane stalk formation, the dominant energy barrier for fusion (*Aeffner et al., 2012*). Upon fusion, the *trans*-SNARE complex becomes a *cis*-complex, anchored to the fused membrane bilayer. Sec17 (α SNAP) and SNAREs are receptors for the Sec18 (NSF) AAA ATPase (*Clary et al., 1990; Winter et al., 2009; Zick et al., 2015*). Sec18 uses the energy from ATP binding and hydrolysis to

disassemble SNAREs for further fusion cycles (Söllner et al., 1993; Ungermann et al., 1998; Zhao et al., 2015) and to disassemble dead-end SNARE complexes (Xu et al., 2010; Lai et al., 2017; Choi et al., 2018; Song and Wickner, 2019; Jun and Wickner, 2019).

The molecular interactions between Sec18/NSF, Sec17/ α SNAP, and neuronal SNAREs were illuminated by determination of their structures when assembled without membrane anchors into the NSF/ α SNAP/SNARE complex, also referred to as the 20S particle (Zhao et al., 2015; White et al., 2018). The heart of these structures is the 4-helical bundle of the R, Qa, Qb, and Qc SNARE domains. Between two and four Sec17/ α SNAP form a right-handed assembly surrounding the left-handed superhelical coiled coils of the SNARE complex. In this structure, the N-terminal apolar loop of each α SNAP is poised to enter a lipid bilayer adjacent to the SNARE transmembrane (TM) domains.

Yeast vacuole fusion, a model of non-neuronal fusion, has been studied in vivo (Wada et al., 1992), in vitro with the isolated organelle (Wickner, 2010), and in a reconstituted proteoliposome-based reaction with purified components (Mima et al., 2008; Stroupe et al., 2009; Zick and Wickner, 2016). Each protein implicated by the in vivo genetics is required for the reconstitution: the Rab Ypt7, the R-SNARE Nyv1, and Q-SNAREs Vam3, Vti1, and Vam7 (hereafter referred to as R, Qa, Qb, and Qc), and a large hexameric protein termed HOPS (homotypic fusion and vacuole protein sorting) with multiple direct affinities. Two HOPS subunits bind Ypt7, anchored on each membrane (Brett et al., 2008), to mediate tethering (Hickey and Wickner, 2010). A third HOPS subunit is Vps33, the vacuolar Sec1/Munc18 (SM) protein, with direct capacity to bind R and Qa SNARE domains, in parallel and in register (Baker et al., 2015). HOPS also has direct affinity for the Qb and Qc SNAREs (Stroupe et al., 2006; Song et al., 2020) and for vacuolar lipids (Orr et al., 2015). Some functions of HOPS correspond to fusion factors in other systems; neuronal Munc13 cooperates with Munc18 in SNARE assembly (Richmond et al., 2001; Ma et al., 2011; Lai et al., 2017). Munc18 corresponds to the HOPS subunit Vps33, but the protein that mediates the Munc13 function for vacuole fusion is unclear. The association of HOPS with Ypt7 and vacuolar lipids allosterically activates HOPS to catalyze SNARE assembly (Torng et al., 2020). When the SNAREs are initially in 4-SNARE complexes on two apposed membranes, fusion requires Sec17, Sec18, and ATP to disassemble these cis-SNARE complexes and liberate the SNAREs for assembly into trans-complexes (Mayer et al., 1996; Nichols et al., 1997; Zick et al., 2015).

Though early studies have suggested that disassembly of cis-SNARE complexes might be the sole function of Sec17 and Sec18 (Mayer et al., 1996), recent findings have broadened our understanding of their roles. While SNAREs are a core fusion machine (Weber et al., 1998), a complete fusion machine (Mima et al., 2008; Zick and Wickner, 2016) also requires the Rab, its tethering effector, an SM-family protein, and the NSF/Sec18 and α SNAP/Sec17 SNARE chaperones. In this more complete context, Sec17 and Sec18 also contribute to fusion per se: (1) trans-SNARE complexes, which form in a Ypt7-dependent manner between vacuoles, bear Sec17 in comparable abundance to the SNAREs (Xu et al., 2010). (2) Fusion between proteoliposomes has been reconstituted with purified components. When tethering is by non-specific agents, fusion is inhibited by Sec17, Sec18, and ATP (Mima et al., 2008; Song et al., 2017). However, Sec17, Sec18, and ATP stimulate fusion with HOPS (Mima et al., 2008; Zick et al., 2015; Song et al., 2017). (3) A pioneering study by Schwartz and Merz, 2009, showed that the Qc3 Δ deletion of several heptads at the C-terminus of the Qc SNARE blocks the fusion of isolated yeast vacuoles, but this block is overcome by the addition of Sec17. Qc3 Δ , ending at the SNARE domain layer +3 and thus lacking layers +4 to +8, blocks vacuole fusion in vivo as well, and overexpression of Sec17 partially restores cellular vacuole morphology (Schwartz et al., 2017). Reconstituted in vitro fusion with limiting Sec17 concentrations, where Sec17 will not restore fusion, also requires Sec18 (Schwartz et al., 2017). It has been unclear whether the Sec17 bypass of this deletion of the C-terminal Qc region is particular to just this one SNARE or is general for any Q-SNARE, and whether Sec17 simply contributes its SNARE-binding energy to the energy of 3-SNARE zippering or whether it drives fusion by other means. (4) Fusion reactions with initially separate SNAREs can require Sec17, and this fusion is stimulated by Sec18 without ATP hydrolysis (Zick et al., 2015; Song et al., 2017). Sec17 alone stimulates the fusion of reconstituted proteoliposomes with wild-type SNAREs, and the degree of stimulation is a function of the lipid headgroup and fatty acyl composition (Zick et al., 2015). An intermediate in fusion accumulates during HOPS-dependent fusion without Sec17, allowing a sudden burst of fusion upon Sec17 addition (Zick et al., 2015). Single-molecule pulling studies have also revealed that α SNAP stabilizes

SNARE complexes (*Ma et al., 2016*, but see *Ryu et al., 2015*). However, the mechanism by which HOPS-dependent fusion is stimulated by Sec17/Sec18 has been unclear.

Complete SNARE zippering is considered essential for SNARE-dependent fusion (*Sørensen et al., 2006*). We now report that Sec17 has a second mode of promoting fusion, which can compensate for incomplete zippering. Fusion with SNAREs and HOPS is completely arrested when several heptad repeats in the C-terminal region of the SNARE core complex are removed from any one of the three Q-SNAREs. With any such C-terminally truncated Q-SNARE domain, or even with C-terminal truncations to both Qb and Qc, blocked fusion is restored by Sec17 and Sec18 without ATP hydrolysis. Association between the C-terminal heptads of the R and the single remaining full-length Qa-SNARE, each anchored to one of the docked membranes, would not yield the same assembly energy as with wild-type SNAREs (*Sutton et al., 1998*) and would contribute far less force toward the bilayer rearrangements of fusion. The N-terminal apolar loop of Sec17 is particularly important for this function of Sec17, and it may stabilize SNARE bundles or trigger fusion by insertion into lipid bilayers. Zippering-driven fusion is also arrested with full-length SNARE domains when the apolar, inward-facing residues of the Qa SNARE layers +4 to +8 are replaced by Ala, Ser, or Gly, but in each case fusion is restored by Sec17, Sec18, and non-hydrolyzable ATP γ S. Strikingly, even fusion that is blocked by the concurrent replacement of apolar residues from the +4 to +8 layers of Qa and the deletion of the +4 to +8 layers of both Qb and Qc, removing all capacity for hydrophobic collapse between the +4 and +8 layers of the R and Q SNAREs, is fully restored by Sec17 and Sec18. We propose that Sec17 either creates a favorable folding environment for the assembly of the remaining full-length SNARE domains or directly promotes bilayer remodeling through insertion of the apolar loops of several SNARE-bound Sec17s or acts by a combination of these two mechanisms.

Results

Vacuole SNAREs (*Figure 1A*) have an N-domain and a SNARE domain. Several of them have a TM anchor, but Qc lacks a hydrophobic membrane anchor, and instead associates with membranes through its affinities for the other SNAREs, for HOPS (*Stroupe et al., 2006*), and for phosphatidylinositol 3-phosphate through its N-terminal PX domain (*Cheever et al., 2001*). SNARE domain layers are numbered from the central 0-layer, as shown. Fusion requires that R- and at least one Q-SNARE be anchored to docked membranes (*Song and Wickner, 2017*). When they are, soluble forms of the other Q-SNAREs without membrane anchors, termed sQ (*Figure 1A*), will support Ypt7/HOPS-dependent fusion. Vacuolar SNAREs with C-terminal truncations, corresponding to partial zippering, form stable complexes (*Figure 1—figure supplement 1*), supporting their use in fusion studies. Based on the single-particle cryo-EM (Electron Microscope) structure of the homologous human neuronal NSF/ α SNAP/SNARE complex (*Zhao et al., 2015*), we modeled the associations of Sec17 (α SNAP) (*Figure 1B*) and Sec18 (NSF) with vacuolar SNAREs, viewed in profile or in an end-on view from the membrane (*Figure 1C*). In this model, we assume that four Sec17 monomers (*Figure 1B*) assemble together, surrounding the 4-SNARE coiled coil (*Figure 1C*). In contrast, only two α SNAP molecules have been observed in EM structures of the NSF/ α SNAP/V7-SNARE complex (*Zhao et al., 2015*) and the NSF/ α SNAP/SNARE complex that included the linker between the two SNAP-25 SNARE domains (*White et al., 2018*). The presence of the SNAP-25 linker in these two complexes may interfere with the binding of the other two α SNAP molecules. Since the vacuolar SNARE complex does not contain a linker between SNARE domains, it is reasonable to postulate that four Sec17 molecules bind to the vacuolar SNARE complex, but the precise number of Sec17 molecules is yet to be determined for the Sec18/Sec17/vacuolar SNARE complex. Rapid fusion needs Sec17 and Sec18 in addition to HOPS and SNAREs (*Song et al., 2017*). To understand how they work together, we exploited direct assays of SNARE associations to show that incompletely zippered SNAREs can associate stably and that HOPS allows Sec17 to promote the completion of zippering and SNARE complex stability. We then examined their functional relationships to show that SNARE-bound Sec17 and Sec18 can promote rapid fusion when energy from zippering is greatly reduced or lost.

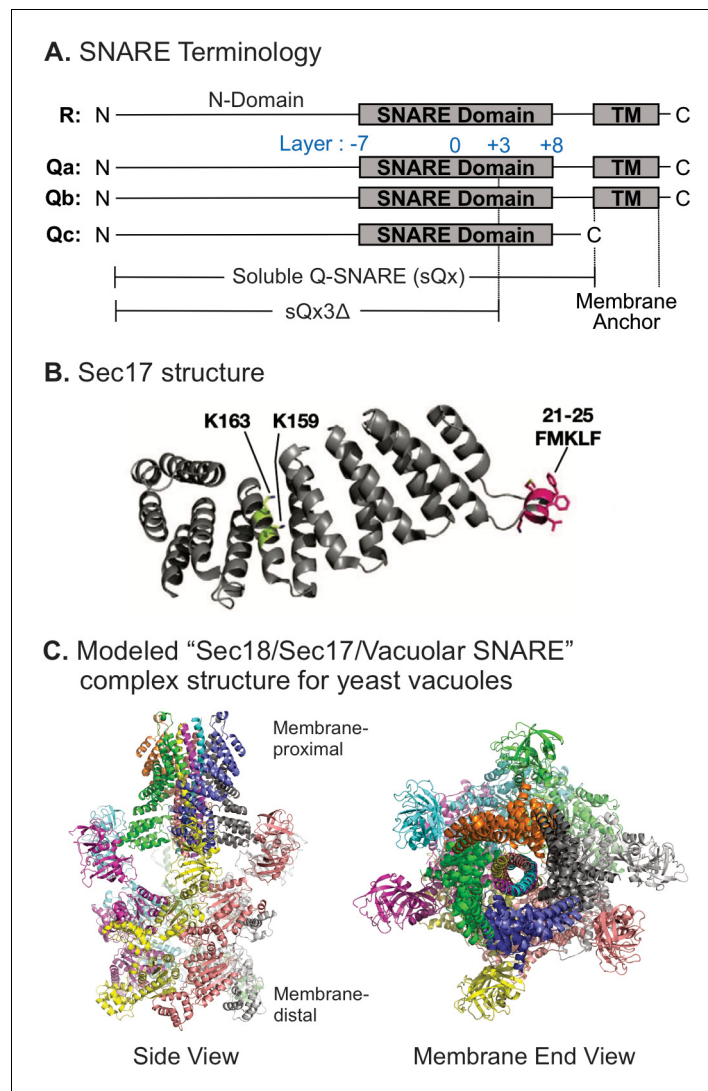


Figure 1. Model of the Sec18/Sec17/vacuolar SNARE complex and Sec17 mutations. **(A)** Schematic of the four yeast vacuolar SNAREs, the soluble Q-SNAREs (sQx), and their deletion derivatives sQx3 Δ lacking regions C-terminal to the +3 layer of the SNARE domain. **(B)** Structure of Sec17 (Rice and Brunger, 1999, PDB ID 1QQE). Residues mutated in certain experiments are highlighted as in Schwartz et al., 2017. **(C)** Modeling of the vacuolar Sec18/Sec17/SNARE complex. MODELLER (Webb and Sali, 2016) was used to create individual homology models of the vacuolar SNARE complex (Nyv1, Vam3, Vti1, Vam7) and of Sec18 starting from the coordinates of synaptobrevin-2, SNAP-25, syntaxin-1A, and NSF in the cryo-EM structure of the neuronal 20S complex (PDB ID 3J96) (Zhao et al., 2015). These homology models, together with the crystal structure of Sec17 (PDB ID 1QQE) (Rice and Brunger, 1999), were fit into the cryo-EM structure of the neuronal 20S complex (PDB ID 3J96) (Zhao et al., 2015). We used PDB ID 3J96 because this cryo-EM structure did not include the SNAP-25 linker and the H_{abc} domain of syntaxin-1A. The vacuolar SNARE complex (Nyv1, Vam3, Vti1, Vam7) also does not include a linker between any of the SNARE motifs; in all structures of NSF/ α SNAP/ternary SNARE complexes determined thus far, four α SNAP molecules are observed for SNARE complexes that do not contain a linker connecting two of the SNARE domains (White et al., 2018), and we therefore included four Sec17 molecules in our model of the vacuolar 20S complex. In the PDB coordinate file supplied as Source Data File of the homology model of the Sec18/Sec17/vacuolar SNARE complex, Sec18 molecules, chains A–F; Sec17, chains G–J; Nyv1, chain K; Vam3, chain L; Vti1, chain M; Vam7, chain N are included. Colors: cyan: Nyv1; magenta: Vam3; yellow: Vti1; salmon: Vam7; gray, orange, green, slate: Sec17; yellow, magenta, gray, blue, salmon, green: Sec18. Cartoon representations are shown. Two views related by a 90-degree rotation are included (left: side view; right: membrane-end view).

© 2017, Schwartz et al. **Figure 1B** reproduced from Figure 5A Schwartz et al., 2017, eLife, published under the Creative Commons Attribution 4.0 International Public License.

Figure 1 continued on next page

Figure 1 continued

The online version of this article includes the following source data and figure supplement(s) for figure 1:

Source data 1. Source data file (PDB) for **Figure 1C**.

Figure supplement 1. SNARE associations during partial zippering.

Sec17 alters SNARE complex conformation

The capacity of vacuolar SNAREs to form stable partially zippered structures raised the question of whether these SNAREs can zipper efficiently, especially when anchored to membranes or associated with other fusion proteins such as HOPS. To study the kinetics of SNARE interactions, we employed an ensemble fluorescence resonance energy transfer (FRET) assay of vacuolar SNARE associations (Torng *et al.*, 2020). The Qc-SNARE was prepared with a unique cysteinyl residue in any of three positions (Figure 2A), either the native Cys208, which is upstream (U) of the SNARE domain or, after substitution of serine for this cysteine, with Met250Cys at the N-terminal end of the SNARE domain or with Ala316Cys at the C-terminal end of the SNARE domain. Each was derivatized with Oregon Green 488. Fusion proteins were also prepared with a unique cysteine either immediately N-terminal, or C-terminal, to the Qb SNARE domain, and each was derivatized with Alexa Fluor 568. As a model for exploring the effects of HOPS and Sec17 on SNARE dynamics, these fluorescent proteins were co-incubated with proteoliposomes bearing Ypt7, R, and Qa. *cis*-SNARE complex assembly can occur spontaneously on these proteoliposomes, but assembly is stimulated by HOPS, allowing direct comparison of HOPS-dependent and HOPS-independent SNARE assembly (Torng *et al.*, 2020). The average FRET efficiency in these studies is modest because they include, in bulk reactions, all the fluorescent Qb and Qc, many of which do not enter SNARE complexes. SNARE complex assembly with HOPS gave a high average FRET efficiency when fluorophores were at the N-terminus of the Qb SNARE domain and at or near the N-terminal end of the Qc SNARE domain (Figure 2B, red and yellow curves). There was a lower FRET efficiency when the fluorophores were at opposite ends of the Qc and Qb SNARE domains (Figure 2B; blue, green, and indigo). When both fluorophores were at the C-terminal ends of the Qb and Qc SNARE domains, a low signal was seen (Figure 2B, purple), similar to the average FRET efficiency when fluorophores were at opposite ends of the SNARE domains, thus suggesting incomplete zippering. After 1 hr, Sec17 was added to each reaction. Strikingly, Sec17 only enhanced the average FRET efficiency between C-terminal fluorophores, rapidly rising to the level seen when the fluorophores were together at the N-termini of the SNARE domains (Figure 2B, purple; Figure 2—figure supplement 1), indicating a Sec17-induced change at the C-terminal end of the SNARE complex. Sec17/ α SNAP may promote the zippering of isolated SNARE domains (Ma *et al.*, 2016) but is now seen to act in the context of membranes and HOPS.

Sec17-induced conformational change requires HOPS

Proteoliposomes with R, Qa, and Ypt7 (where indicated) were incubated with Qb-SNARE domain and Qc. Both SNARE domains were either fluorescently labeled at their N-termini (Figure 2C, bars 1–5) or at their C-termini (Figure 2C, bars 6–10). Incubations were in the presence or absence of HOPS. Sec17 addition after 1 hr did not enhance the average FRET efficiency between N-terminally disposed fluorophores in the presence or absence of HOPS (Figure 2C, bars 1–5), but stimulated the average FRET efficiency between SNARE domain C-terminal fluorophores in a HOPS-dependent manner (Figure 2C, bars 6–10), since the enhanced FRET between the SNAREs in the presence of HOPS and Sec17 (bar 9) is not seen without HOPS (bar 8) or without Sec17 (bar 10). This indicates a HOPS-dependent and Sec17-induced SNARE conformational change. This was diminished when zippering was inhibited by the absence of the +4 to +8 layers of sQa (Figure 2D, bar 1 vs. 3) or by the conversion of each inward-facing apolar residue of the full-length Qa SNARE domain layers +4 to +8 to Gly (Figure 2E, bar 1 vs. 3). The F22SM23S mutation of Sec17 (FSMS hereafter), diminishing the hydrophobicity of its N-domain loop (Song *et al.*, 2017), reduced the Sec17 capacity for inducing HOPS-dependent conformational change (Figure 2F). We also examined the effects of other mutants of Sec17. The K159E,K163E mutation (KEKE hereafter) diminishes Sec17:SNARE association (Marz *et al.*, 2003); one of these residues (Sec17 K159) is in a pair (α SNAP K122, K163) that abolishes disassembly of the neuronal SNARE complex by NSF/ α SNAP (Zhao *et al.*, 2015). The

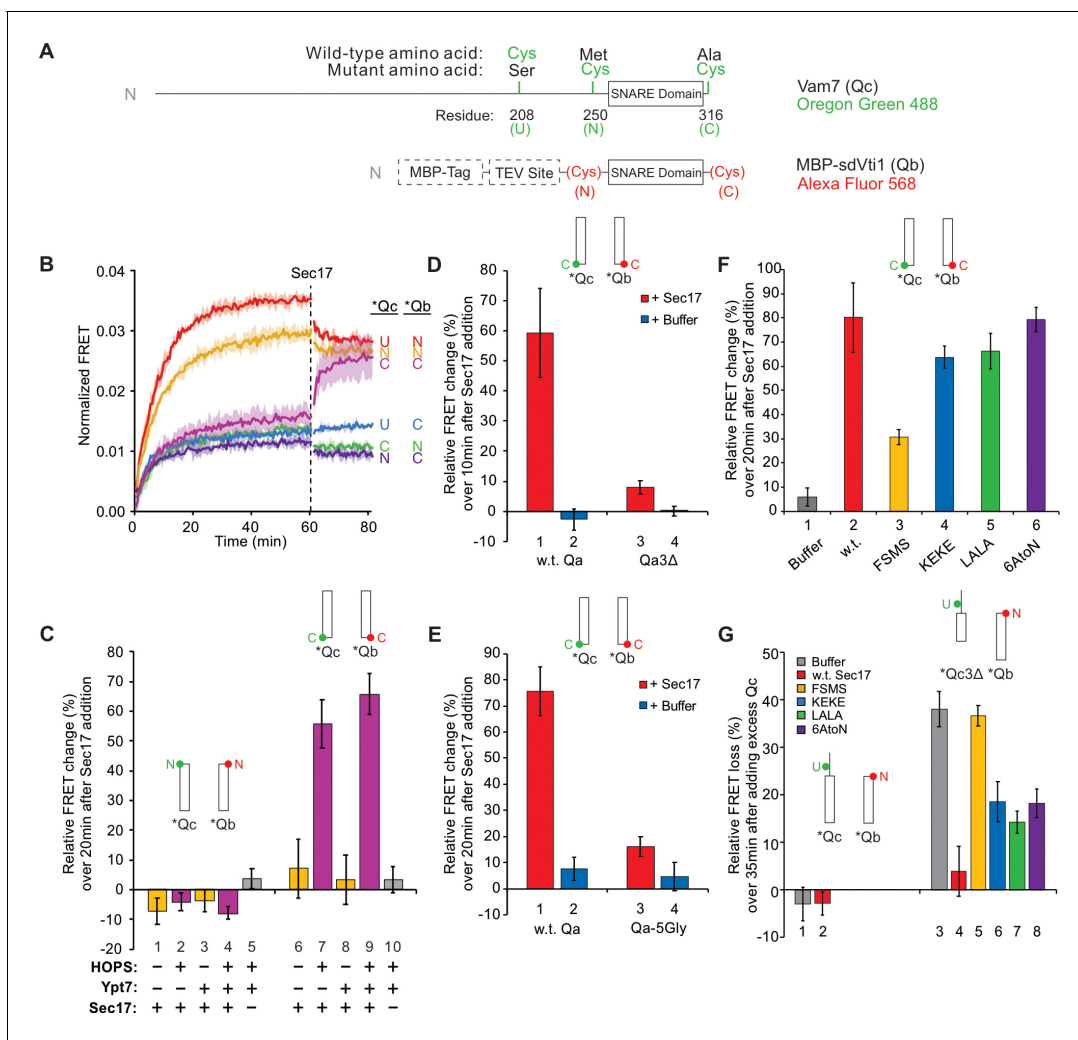


Figure 2. Sec17 modifies SNARE conformation in a HOPS- and zippering-dependent manner and stabilizes complexes with truncated SNARE domains. (A) Schematic of fluorescently labeled SNARE constructs used in this study. SNAREs were derivatized as described previously (Tornig et al., 2020). Wild-type Qc contains a single Cys residue at 208 at the upstream (U) position. (N)- and (C)-labeled constructs replace residues 250 and 316 with Cys, while also replacing Cys208 with Ser. Each Qc construct was derivatized with Oregon Green 488 as described (Tornig et al., 2020). A fusion of maltose-binding protein (MBP), a TEV site, and the Qb SNARE domain (residues 133–187) was expressed with an added cysteinyl residue immediately upstream or downstream of the SNARE domain. Each Qb construct was derivatized with Alexa Fluor 568. Qc and Qb labeled with a fluorescent probe at any position are written as *Qc and *Qb. (B–G) Bar graphs are reported as the mean of the relative ensemble fluorescence resonance energy transfer (FRET) change (%) per trial with propagated standard deviation for $n = 3$ trials. The relative change was calculated by averaging 10 data points, each from just before Sec17 addition and from the end of the measurement period 20 min later, except where indicated. Specific time points used as well as the statistics for the propagation of uncertainty are shown in Supplementary Data. A bar graph representation for (B) and the kinetic curves for (C–G) are provided in **Figure 2—figure supplement 1**. (B) Sec17 modifies the conformation of the C-terminus of the SNARE complex. Ypt7/RQa proteoliposomes were incubated with pairs of *Qb and *Qc labeled at the N, C, or upstream (U) locations as indicated in (A). Curves are averages of $n = 3$ trials, and the shaded regions behind each curve show the standard deviation per time point. (C) Sec17-promoted zippering requires HOPS. RQa proteoliposomes were incubated with either the N-labeled *Qb/*Qc pair (left) or the C-labeled *Qb/*Qc pair (right), with Ypt7 and HOPS as indicated. A reaction with a buffer (RB150) added instead of Sec17 serves as a negative control. (D) Sec17 does not promote C-terminal zippering if the SNARE domain of Qa is truncated. Ypt7/R proteoliposomes were incubated with C-terminally labeled *Qb and *Qc and either soluble Qa or Qa3Δ, and the relative FRET change was calculated over 10 min after Sec17 or buffer addition. (E) Sec17-induced zippering requires the apolar heptad-repeat amino acyl residues in Qa SNARE domain layers +4 to +8. Proteoliposomes bearing Ypt7, R-SNARE, and either wild-type Qa or Qa with the +4 to +8 layers inwardly-oriented apolar residues mutated to Gly were incubated with C-terminally labeled *Qb and *Qc, and then Sec17 or its mutants were added at $t = 60$ min. (F) Sec17-driven SNARE conformational change is stunted by the F225M23S mutation of Sec17 (FSMS). Ypt/R proteoliposomes were incubated with sQa and C-terminally labeled *Qb and *Qc, and then Sec17 or mutants as indicated were added at $t = 60$ min. (G) Sec17 stabilizes incompletely zippered SNARE complexes. Ypt7/R proteoliposomes were incubated with sQa and C-terminally labeled *Qb and *Qc. Sec17 or the indicated mutants were added at $t = 60$ min. Non-fluorescent Qc (8.5 μ M) was added at $t = 80$ min, and the loss of FRET over 35 min was measured starting immediately after the addition of non-fluorescent Qc.

Figure 2 continued on next page

Figure 2 continued

The online version of this article includes the following source data and figure supplement(s) for figure 2:

Source data 1. Source data file (Excel) for **Figure 2B**.**Figure supplement 1.** Statistics and representative kinetic data for **Figure 2**.**Figure supplement 2.** Direct binding of Sec17 to HOPS.

C-terminal L291A,L292A mutation of Sec17 (LALA hereafter) interferes with its cooperation with Sec18 for SNARE complex disassembly (Barnard *et al.*, 1997; Schwartz and Merz, 2009; Zick *et al.*, 2015), and 6AtoN is the conversion of six inward-facing acidic residues of Sec17, which face basic SNARE residues in the 20S structure (Figure 1C), to neutral residues. Neither KEKE, LALA, nor 6AtoN had a large effect on the capacity of Sec17 to promote HOPS-dependent conformational change (Figure 2F).

Since this Sec17-induced SNARE conformational change is seen with C-terminal fluors but not with N-terminal fluors, requires HOPS as the SNARE assembly catalyst, and requires SNAREs that can zipper, a major part of the conformational change may be zippering itself. This might be spontaneous after Sec17-induced release of HOPS from SNAREs (Collins *et al.*, 2005; Schwartz *et al.*, 2017) or be promoted by Sec17 binding along the SNAREs (Figure 1C), reflecting its affinity for the C-terminal region of SNARE bundles (Ma *et al.*, 2016). HOPS bound to SNAREs may inhibit C-terminal zippering, even though it helps to assemble the N-terminus of the four-helix bundle. Sec17 could then increase FRET because it displaces HOPS. Such C-terminal zippering would be favored by Sec17 binding, but could also be spontaneous in the absence of these factors.

Sec17 also interacts with partially zippered SNARE complex to promote SNARE complex stability. SNARE complex was assembled by HOPS on Ypt7/R proteoliposomes with soluble Qa, with the Qb SNARE domain labeled with a fluorophore at a cysteinyl residue upstream of the SNARE domain, and with Qc of full length (w.t.) or with the 3Δ C-terminal truncation, each bearing a fluorophore at its native cysteinyl residue upstream of the SNARE domain. When the complex of proteoliposomes with these fluorescent Qb and Qc had full-length SNARE domains, it was stable whether or not it included Sec17, as there was no loss of average FRET efficiency after addition of excess non-

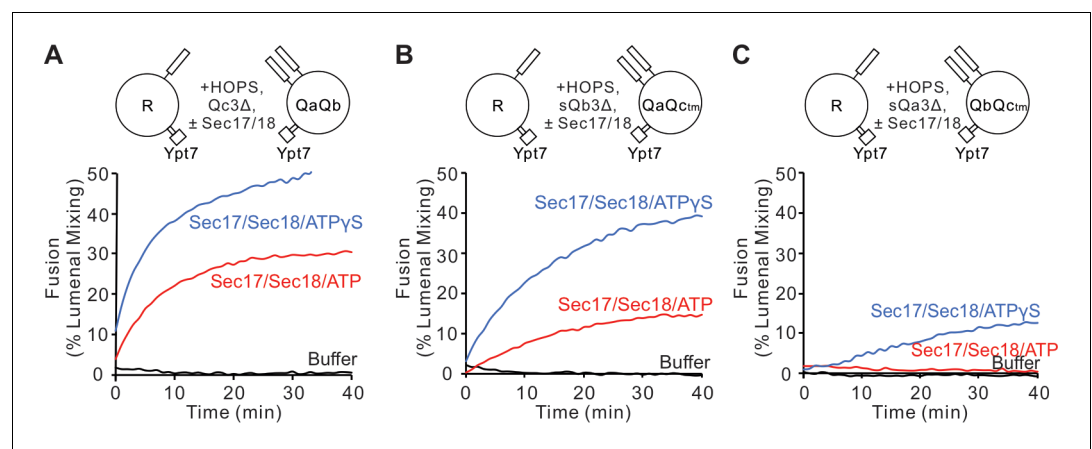


Figure 3. Fusion is blocked by deletion of the last five C-terminal SNARE domain layers from any single Q-SNARE and is restored by Sec17, Sec18, and ATP or ATPγS. (A) Fusion incubations, as described in 'Materials and methods', had Ypt7/R and Ypt7/QaQb proteoliposomes (1:8000 Ypt7:lipid molar ratio, 1:16,000 SNARE:lipid molar ratio), 2 μM Qc3Δ, and, where indicated, 600 nM Sec17, 300 nM Sec18, 1 mM ATP (red), or ATPγS (blue). (B) Fusion with 2 μM sQb3Δ and with Ypt7/QaQc_{tm} proteoliposomes, but otherwise as in (A). (C) Fusion with 2 μM sQa3Δ and with Ypt7/QbQc_{tm} proteoliposomes, but otherwise as in (A). Mean and standard deviations from three independent experiments are shown in **Figure 3—figure supplement 1**. The online version of this article includes the following source data and figure supplement(s) for figure 3:

Source data 1. Source data file (Excel) for **Figure 3A,B and C**.**Figure supplement 1.** Statistics for **Figure 3**.

fluorescent Qc (**Figure 2G**, bars 1 and 2; **Figure 2—figure supplement 1G**). In contrast, fluorescent Qc3Δ was 'chased' by exchange with non-fluorescent Qc (bar 3), but Sec17 stabilized this SNARE complex, blocking the chase (bar 4). Thus, in the absence of Sec17, the assembly of Qc3Δ into partially zippered SNARE complex is reversible. Each domain of Sec17 helps to stabilize Qc3Δ against exchange (bars 5–8), especially the Sec17 N-terminal apolar loop (bar 5). The HOPS-dependent functions of Sec17, such as promotion of zippering, may be aided by the direct affinity between these proteins (**Figure 2—figure supplement 2**).

Generality of Sec17 and Sec18 bypass of arrested zippering

Sec17 can restore fusion when Qc has truncations at the C-terminal end of its SNARE domain (**Schwartz and Merz, 2009**), stimulated by Sec18 (**Schwartz et al., 2017**). We asked whether Sec17 can restore fusion with similar deletions of residues after the +3 layer in the other Q-SNAREs. Proteoliposomes bearing Ypt7 and R-SNARE were assayed for fusion with proteoliposomes bearing this Rab and any two anchored Q-SNAREs. Proteoliposome mixtures were incubated with HOPS, and the soluble form of the remaining Q-SNARE was deprived of its membrane anchor and a C-terminal portion of its SNARE domain (**Figure 3**; A, Qc3Δ; B, sQb3Δ; C, sQa3Δ). As reported by **Schwartz et al., 2017**, there was no fusion with Qc3Δ unless 600 nM Sec17, 300 nM Sec18, and ATP or ATPγS were present (**Figure 3A**); these concentrations are in the physiological concentration ranges of Sec17 (150–1100 nM) and Sec18 (250–760 nM) (**Ho et al., 2018**). While ATP and its non-hydrolyzable analog ATPγS support comparable fusion with wild-type SNAREs (**Song et al., 2017**), hydrolyzable ATP inhibits fusion through Sec17/Sec18-mediated disassembly of SNARE complexes when defective SNAREs such as Qc3Δ are present, a proofreading function. The same pattern was seen for fusion with sQb3Δ (**Figure 3B**) and sQa3Δ (**Figure 3C**). The unique spatial disposition of the Sec17/αSNAP molecules with respect to each SNARE (**Figure 1C** and **Zhao et al., 2015**) makes it unlikely that Sec17 could somehow fill each of the gaps left by each of these deletions to shield apolar residues within the SNARE bundle and thereby continue to drive zippering, or that Sec17 binding could induce the remaining R and two Q +4 to +8 layers to somehow rotate to form a hydrophobic two- or three-layered core.

Fusion assays were also performed with Ypt7/R proteoliposomes and each of the three Ypt7/single-anchored Q-SNARE proteoliposomes in the presence of HOPS and the other two soluble Q-SNAREs (**Figure 4**). With membrane-anchored Qa and with sQb and Qc having complete SNARE domains, there was HOPS-dependent fusion without further addition (**Figure 4A**, black line), though Sec17 and Sec18 with AMP-PNP, ATPγS, or ATP did stimulate (compare black curves, A–D). Deletion of the +4 to +8 layers from either soluble Qb or Qc abolished fusion (**Figure 4A**), which was restored by Sec17 and Sec18 with either AMP-PNP, ATPγS, or ATP (B–D, red and blue curves). There was no fusion when both soluble Q-SNAREs had truncated SNARE domains (**Figure 4A**, orange), but, strikingly, the fusion was partially restored by Sec17 and Sec18 with ATP (**Figure 4D**, orange) and more fully restored when the adenine nucleotide was resistant to hydrolysis (**Figure 4**, B and C, orange). With two Q-SNAREs lacking the C-terminal portion of their SNARE domains, the apolar amino acyl residues of the remaining two SNAREs would not be as effectively shielded from water if they continued zippering together. Fusion could not be restored by Sec17 and Sec18 if either soluble SNARE was omitted instead of truncated (green and purple). This fusion with sQb3Δ and Qc3Δ occurs in stages, initially sensitive to antibody to either the HOPS SM subunit Vps33 or Sec18, then acquiring resistance to Vps33 antibody while remaining sensitive to the Sec18 ligand (**Figure 4—figure supplement 2**). When only the Qb-SNARE was membrane anchored, there was little fusion without Sec17 and Sec18 (**Figure 4E**, black curve). When the SNARE domain of sQa or Qc had been truncated, fusion was strictly dependent on non-hydrolyzable ATP analogs, and little fusion was seen with dual SNARE domain truncation. Similar patterns were seen with anchored Qc (**Figure 4**, I–L). We term the fusion induced by Sec17 and Sec18 in the presence of 3Δ SNARE domain truncations 'zippering bypass fusion'.

To explore the capacity of Sec17 and Sec18 to compensate for partial SNARE zippering, we assayed the fusion of Ypt7/R and Ypt7/Qa proteoliposomes with sQb3Δ, Qc3Δ, and HOPS, using various concentrations of wild-type or mutant Sec17, and with or without Sec18 and ATPγS (**Figure 5**). Without Sec17, fusion is not supported by Sec18 (A and B, blue curves). Limited fusion is possible with 1 or 2 μM wild-type Sec17 alone (A, black and red), but Sec18 allows faster fusion and with less Sec17 (A and B; tan). Fusion requires the apolar loop near the N-terminus of Sec17, as the

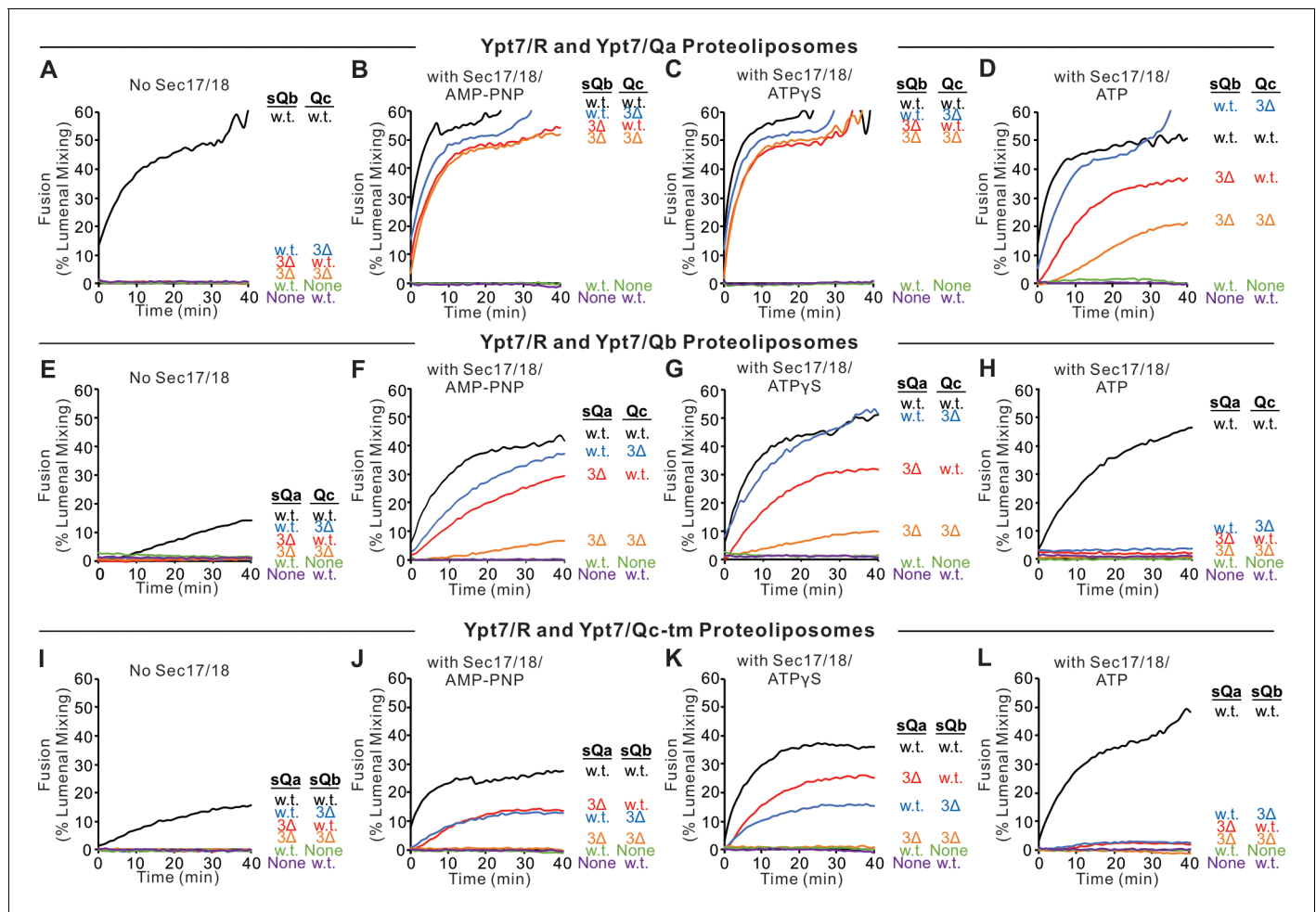


Figure 4. Fusion with single membrane-anchored Q-SNAREs. (A–D) Fusion incubations, as described in ‘Materials and methods’, had Ypt7/R and Ypt7/Qa proteoliposomes (1:8000 Ypt7-TM:lipid molar ratio, 1:16,000 SNARE:lipid molar ratio), 50 nM HOPS, 2 μ M sQb or sQb3 Δ , 2 μ M Qc or Qc3 Δ , and, where indicated, 600 nM Sec17, 300 nM Sec18, and 1 mM ATP, AMP-PNP, or ATP γ S. (E–H) Fusion incubations as for (A), but with Ypt7/Qb proteoliposomes and 2 μ M sQa or sQa3 Δ , 2 μ M Qc or Qc3 Δ and Sec17, Sec18, and adenine nucleotide as indicated. (I–L) Fusion incubations as for (A), but with Ypt7/Qc-tm proteoliposomes and 2 μ M sQa or sQa3 Δ , 2 μ M Qb or sQb3 Δ and Sec17, Sec18, and adenine nucleotide as indicated. Mean and standard deviations from more than three independent experiments are shown in **Figure 4—figure supplement 1**. The online version of this article includes the following source data and figure supplement(s) for figure 4:

Source data 1. Source data file (Excel) for **Figure 4A–L**.

Figure supplement 1. Statistics data for **Figure 4**.

Figure supplement 2. Selective inhibitors reveal successive fusion intermediates.

F21S,M22S mutation (FSMS) blocks fusion entirely (C and D). The K159E,K163E mutation (KEKE) diminishes Sec17:SNARE association (*Marz et al., 2003*). The KEKE mutation prevents fusion without Sec18 (E), but a slow and limited fusion with KEKE-Sec17 is restored by Sec18 (F). The C-terminal L291A,L292A mutation of Sec17 (LALA), which interferes with its cooperation with Sec18 for SNARE complex disassembly (*Barnard et al., 1997; Schwartz and Merz, 2009; Zick et al., 2015*), diminishes zippering bypass fusion (A vs. G, red curves), and a limited fusion is restored through the addition of Sec18 (H). These data suggest that Sec17 action directly requires its apolar loop domain, since the loss of this apolar region is not bypassed by Sec18. Sec18 may stimulate fusion by modulating the conformation of Sec17 associations with *trans*-SNARE complexes, but Sec18 is not simply promoting Sec17 binding, since it is still needed for fusion when Sec17 is joined to an integral N-terminal membrane anchor (**Figure 5—figure supplement 2**). Basic residues in the +3 to +8 layers near the C-terminus of the R and Qa SNARE domains are near acidic residues on the interior of the Sec17 assembly (**Figure 5I**). To determine whether Sec17 might rely on these ionic interactions to support

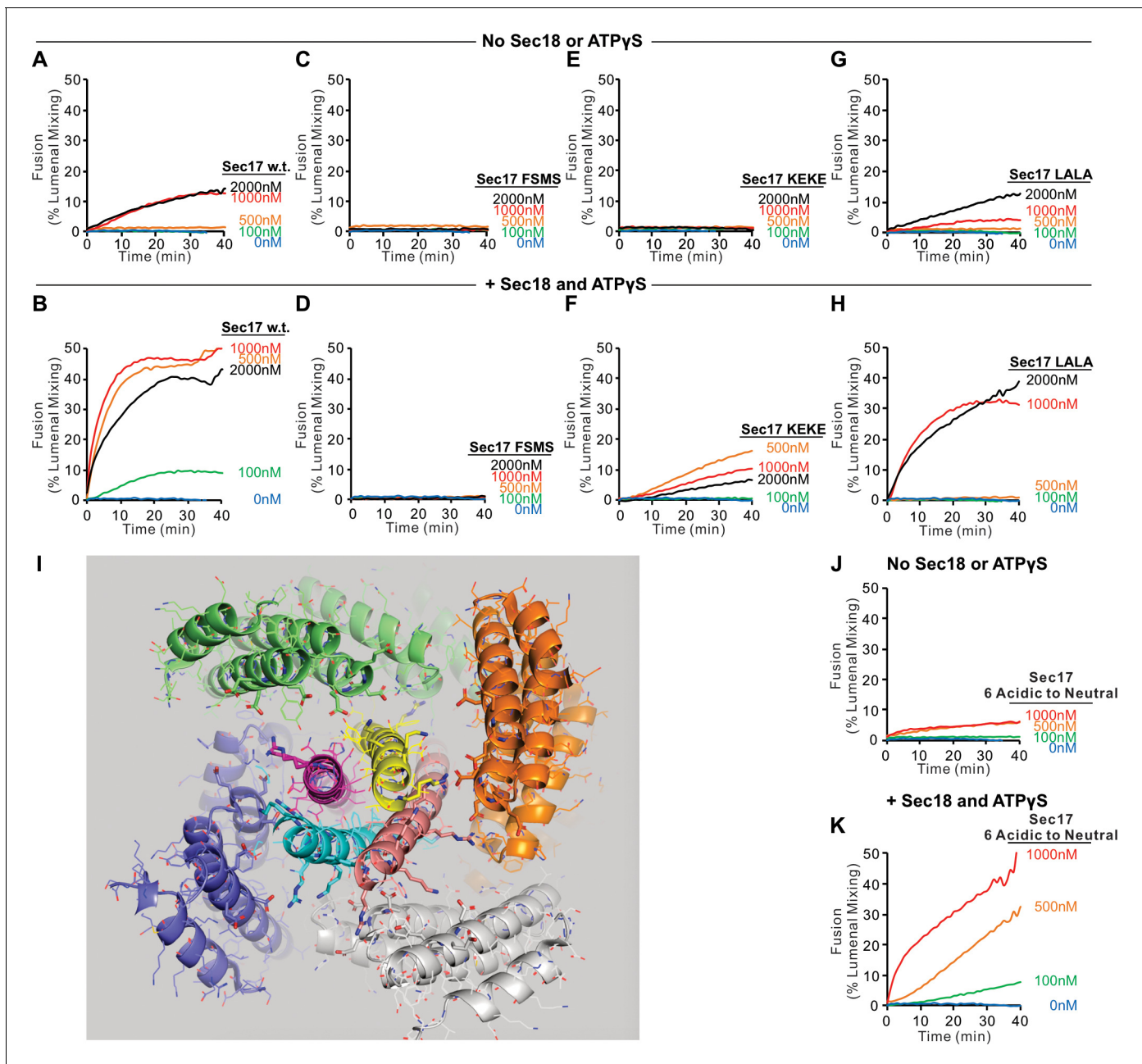


Figure 5. Role of each domain of Sec17 in zippering bypass fusion. (A-H, J, K) Fusion between Ypt7/R and Ypt7/Qa proteoliposomes (1:8000 Ypt7-TM:lipid and 1:16,000 SNARE/lipid molar ratios) was assayed with 50 nM HOPS, 2 μ M sQb3 Δ , 2 μ M Qc3 Δ , the indicated concentration of wild-type or mutant Sec17, and with or without 250 nM Sec18 and 1 mM ATP γ S. (I) Ionic interactions between Sec17s and vacuolar SNAREs in the +4 to +8 layers in the model of the Sec18/Sec17/vacuolar SNARE complex (**Figure 1**). Colors: cyan: R; magenta: Qa; yellow: Qb; salmon: Qc; gray, orange, green, slate: Sec17; red: oxygen atoms; blue: nitrogen atoms. Cartoon representations are shown along with side chains shown as thin lines. Thick lines (sticks) are interacting glutamate and aspartate (acidic) residues on the surface of Sec17 (aminoacyl residues 34, 35, 38, 73, 74, 75) that interact with the vacuolar SNARE complex lysine and arginine basic residues in each of the four SNAREs. Mean and standard deviations from four independent experiments are shown in **Figure 5—figure supplement 1**.

The online version of this article includes the following source data and figure supplement(s) for figure 5:

Source data 1. Source data file (Excel) for **Figure 5A–H, J and K**.

Figure supplement 1. Mean and standard deviations of fusion after 60 min from four independent assays as in **Figure 5** are shown.

Figure supplement 2. Sec18 does not simply promote fusion by contributing to the affinity of Sec17 for membranes that bear SNARE complexes.

fusion, we converted these acidic residues of Sec17 to alanine or serine, creating the mutant Sec17-E34S,E35S,D38S,E73A,D74A,E75A (termed Sec17 6 Acidic to Neutral or Sec17-6AtoN), but this mutant Sec17 still supports fusion (**Figure 5**, J and K). Interestingly, mutation of acidic residues of α SNAP near the C-terminal end of the neuronal SNARE complex also only had a modest effect on disassembly activity of NSF/ α SNAP (**Zhao et al., 2015**).

Fusion despite triply-crippled SNARE zippering

Since SNARE zippering is driven by the sequestration of apolar residues into the interior of the 4-SNARE bundle, we examined the effect of converting the apolar residues of the Qa SNARE domain +4 to +8 layers to Ala, Ser, or Gly. Fusion between Ypt7/R and Ypt7/Qa proteoliposomes in the presence of HOPS, sQb, and Qc, but without Sec17 or Sec18 (**Figure 6A**, black curve), was diminished by replacing each of the +4 to +8 layer apolar residues of Qa with Ala (**Figure 6A**, green curve) and was abolished when they were replaced by Ser (red curve) or by Gly (blue curve). The persistence of some fusion with the Ala substitutions may reflect that two of the residues were already Ala, that Ala has the greatest propensity among the amino acids to form α -helices, Gly the least, and Ser is in-between (**Pace and Scholtz, 1998**), and that alanine itself is the least hydrophilic of these three amino acids. When these same incubations were performed with Sec17, Sec18, and ATPyS, rapid and comparable fusion was seen in each case (**Figure 6B**). When hydrolyzable ATP was

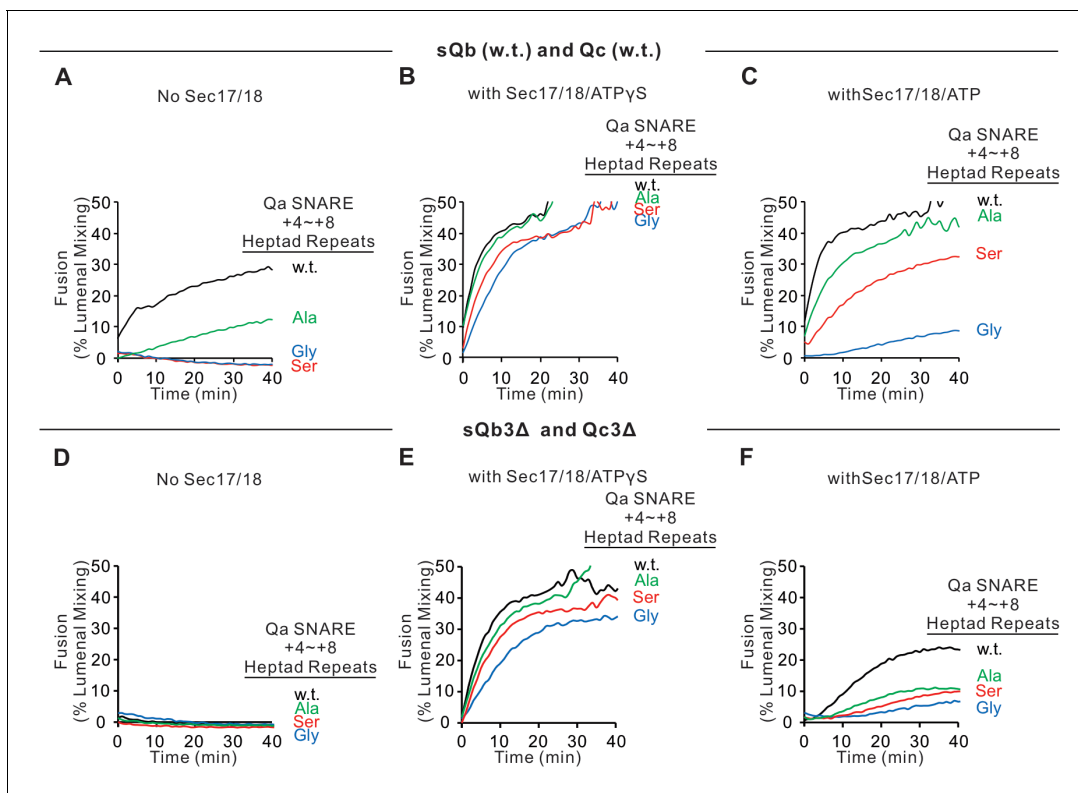


Figure 6. Sec17, Sec18, and ATPyS restore fusion to Ypt7/R and Ypt7/Qa proteoliposomes, which were triply-crippled from completion of SNARE domain zippering by deletion of the +4 to +8 layers of the sQb and Qc SNAREs and by substitution of the apolar residues of the +4 to +8 layers of Qa, substituting Ala, Ser, or Gly for L238, M242, A245, L249, and A252. Fusion incubations ('Materials and methods') had (A–C) Ypt7/R and Ypt7/Qa (w.t. (black), Gly mutant (blue), Ser mutant (red), or Ala mutant (green)) proteoliposomes (1:8000 Ypt7-TM:lipid molar ratio, 1:16,000 SNARE:lipid molar ratio), 50 nM HOPS, 2 μ M sQb (w.t.), and 2 μ M Qc (w.t.) (A–C) or (D–F) 2 μ M Qc3 Δ and 2 μ M sQb3 Δ . Sec17 and Sec18 buffers (A and D) or 600 nM Sec17, 300 nM Sec18, and 1 mM ATPyS (B and E) or ATP (C and F) were also present. Kinetics shown are representative of four experiments. Mean and standard deviations from four independent experiments are shown in **Figure 6—figure supplement 1**. The online version of this article includes the following source data and figure supplement(s) for figure 6:

Source data 1. Source data file (Excel) for **Figure 6A–F**.

Figure supplement 1. Fusion assays between Ypt7/R- and Ypt7/Qa with Qa w.t. (black), Qa 5Ala mutant (green), Qa 5Gly mutant (blue), or Qa 5Ser mutant (red) as described in **Figure 6**.

used instead of ATP γ S, there was little effect on the fusion kinetics with wild-type SNARE domain sequences (**Figure 6**, B vs. C, black curves). In contrast, hydrolyzable ATP led to fusion inhibition when SNARE packing stability was reduced by substitution of apolar residues by Ala, Ser, or Gly (**Figure 6C**). Though the apolar residues are not required for fusion aided by Sec17 and Sec18 (**Figure 6B**), they apparently stabilize the SNAREs against ATP-driven proofreading disassembly (**Figure 6C**). To triply weaken the completion of zippering, the same proteoliposomes with wild-type Qa or the Qa with +4 to +8 layers having small side-chain residues instead of apolar residues were incubated with HOPS, sQb3 Δ , and Qc3 Δ , either without Sec17 or Sec18 (**Figure 6D**) or with Sec17, Sec18, and ATP γ S (**Figure 6E**) or ATP (**Figure 6F**). Fusion was optimally supported by Sec17, Sec18, and ATP γ S (**Figure 6E**). The independence of this fusion from energy derived by zippering is underscored by the similar fusion rates in all incubations with Sec17, Sec18, and ATP γ S, whether with apolar or polar Qa +4 to +8 residues or with full-length or +4to +8-truncated sQb and Qc (**Figure 6**, B vs. E). With the Qb and Qc SNARE domains truncated, and the Qa lacking apolar inward-facing amino acyl side chains, little or no energy could be gained from the completion of R and mutant-Qa zippering. Thus, Sec17 acts in three ways: triggering a zippering-dependent SNARE conformational change in the presence of HOPS and full-length SNARE domains (**Figure 2**), acting with Sec18 to promote fusion independent of energy from zippering (**Figure 6**), and supporting the disassembly of post-fusion *cis*-SNARE complexes by Sec18.

Discussion

The catalytic roles of fusion proteins have been gleaned from functional reconstitution studies. These studies initially showed that the zippering of concentrated SNAREs can drive slow fusion (**Weber et al., 1998; Fukuda et al., 2000**). As proteoliposome SNARE levels were lowered toward physiological levels, reconstituted vacuolar and neuronal fusion reactions required additional factors (**Zick and Wickner, 2016; Stepien and Rizo, 2021**). In addition to SNAREs, reconstituted neuronal fusion requires Munc18, Munc13, calcium, NSF, and α SNAP (**Ma et al., 2013; Lai et al., 2017**) while reconstituted vacuole fusion needs HOPS (**Stroupe et al., 2006**), the Rab Ypt7 (**Stroupe et al., 2009; Ohya et al., 2009**), and specific lipid head-group composition and fatty acyl fluidity (**Zick and Wickner, 2016**). HOPS and other SM proteins catalyze SNARE assembly (**Baker et al., 2015; Orr et al., 2017; Jiao et al., 2018**), regulated by an activated Rab (**Zick and Wickner, 2016; Torng et al., 2020**), and may confer resistance to Sec17/ α SNAP- and Sec18/NSF-mediated *trans*-SNARE disassembly (**Xu et al., 2010; Jun and Wickner, 2019**). Sec17/ α SNAP and Sec18/NSF stimulate fusion with HOPS and wild-type SNAREs (**Mima et al., 2008; Song et al., 2017**).

Fusion can be supported by either complete 4-SNARE zippering without Sec17 or Sec18, or by Sec17 and Sec18 association with only partially zippered SNAREs, but the most rapid fusion requires both (**Song et al., 2017**). While Sec17 and Sec18 are known to bypass the fusion blockade by Qc C-terminal truncation alone (**Schwartz and Merz, 2009; Schwartz et al., 2017**), the generality of this bypass with respect to any one Q-SNARE or even two Q-SNAREs (**Figures 3 and 4**) shows that it is not specific to Qc alone. Moreover, when zippering with full-length SNARE domains is weakened by the substitution of small amino acyl residues for large apolar residues in the +4 to +8 layers of Qa, Sec17 and Sec18 will also restore fusion (**Figure 6A,B**). Strikingly, Sec17 and Sec18 drive fusion despite a triple blockade to complete zippering, namely the absence of two C-terminal Q-SNARE domains and the lack of apolarity in the third (**Figure 6E**). In the NSF/ α SNAP/SNARE complex, the 4-SNAREs wrap around each other in a left-handed super helix, and the Sec17s wrap around them in a right-handed fashion, yet they form a specific structure (**Zhao et al., 2015; White et al., 2018**). It seems unlikely that residues from one or more Sec17 could substitute for the missing residues when two heptads are removed from the C-termini of one or even two Q-SNAREs and the bulky apolar residues are removed from the third.

From the earliest reconstitutions of HOPS-dependent fusion (**Mima et al., 2008**) and in subsequent studies (e.g., **Zick et al., 2015**), Sec17 and Sec18 gave strong stimulation. In contrast, Sec17 and Sec18 inhibit SNARE-only fusion, or fusion with non-physiological tethers (**Mima et al., 2008; Zick and Wickner, 2014; Schwartz et al., 2017; Song and Wickner, 2019**). HOPS not only binds each SNARE, but also has direct affinity for Sec17 (**Figure 2—figure supplement 2**). In model studies with *cis*-SNARE complexes, HOPS is necessary for Sec17 to enhance zippering per se

(Figure 2C). HOPS:Sec17 binding may underlie their synergy for fusion, but further studies are needed to test this idea.

Earlier studies and our current work suggest a working model of vacuole membrane fusion, encompassing findings here and elsewhere (Figure 7). HOPS exploits the affinity of its Vps39 and Vps41 subunits for the Rab Ypt7 (Brett et al., 2008) on each fusion partner membrane (Figure 7A) to mediate (Step 1) tethering (Hickey and Wickner, 2010). Tethered membranes (Figure 7B) are a prerequisite for SNARE assembly in an active conformation, likely a common N to C SNARE domain orientation (Song and Wickner, 2019). HOPS has direct affinity for each of the four vacuolar SNAREs (Song et al., 2020) and is allosterically activated by vacuolar lipids and Ypt7:GTP (Torng et al., 2020) as a catalyst of SNARE assembly (Step 2). SNAREs begin to zipper (Figure 7C) from the N- toward the C-terminal end of their SNARE domain. When any one Q-SNARE is omitted, fusion intermediates assemble, which undergo very rapid fusion when the missing Q-SNARE is supplied (Song et al., 2020), suggesting that fusion without Sec17/Sec18 is rate-limited by the

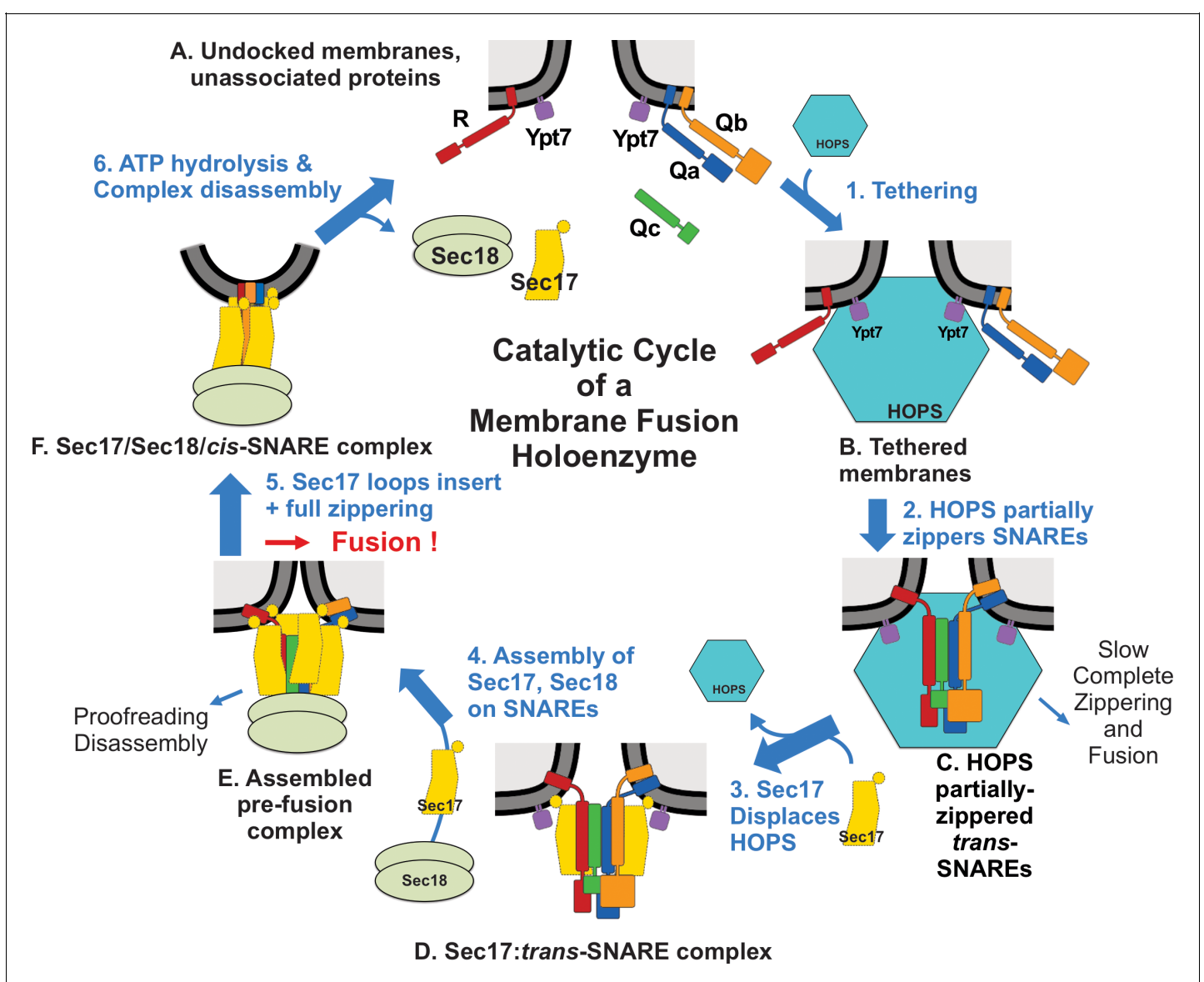


Figure 7. Current working model. Catalyzed tethering and SNARE assembly (A–C) is followed by HOPS displacement by Sec17 (C and D) and further assembly of Sec17 and Sec18 on the partially zippered SNARE complex, promoting completion of zippering and apolar Sec17 loop insertion (D–F), both of which promote fusion. See text for discussion.

completion of SNARE zippering and/or the spontaneous release of bulky HOPS. Sec17 has direct affinity for SNAREs (Söllner *et al.*, 1993), HOPS (Figure 2—figure supplement 2), lipids (Clary *et al.*, 1990; Zick *et al.*, 2015), and Sec18 (Söllner *et al.*, 1993). Sec17 displaces HOPS from the SNAREs (Figure 7, Step 3), as shown by earlier studies: (1) vacuolar SNAREs are found in complex with Sec17 or HOPS, but not with both, and Sec17 can displace HOPS from SNAREs (Collins *et al.*, 2005); (2) when vacuolar HOPS-dependent reconstituted fusion is arrested by Qc3Δ, HOPS is bound to the incompletely zippered SNARE complex until it is displaced by Sec17 (Schwartz *et al.*, 2017); and (3) *trans*-SNARE complexes, which assemble between isolated vacuoles, are largely associated with Sec17 (Xu *et al.*, 2010). The Sec17 association with partially zippered *trans*-SNARE complex (Figure 7D) promotes a conformational change (Figure 2) leading to complete zippering. The Sec17: 4-SNARE complex will bind Sec18 (Step 4) through its affinities for both SNAREs (Zick *et al.*, 2015) and for Sec17. Sec18 regulates, in some unknown fashion, the Sec17/αSNAP assembly into an oligomeric structure surrounding the SNARE complex intermediate (Zhao *et al.*, 2015), a *trans*-anchored Sec18/Sec17/SNARE pre-fusion complex (Figure 7E). Some ATP hydrolysis-dependent disassembly can occur, which may represent proofreading of incorrect and unstable *trans*-SNARE complexes (Choi *et al.*, 2018). Sec17 oligomerization may also be stabilized or guided by the insertion of its N-terminal loop into the membranes. While SNAREs can slowly complete zippering and support fusion without Sec17 or Sec18 (Mima *et al.*, 2008; Song *et al.*, 2017), and slow fusion can occur with Sec17 and Sec18 when sQb and Qc lack the C-terminal portion of their zippering domain (Figure 4D), optimal fusion requires four complete SNARE domains, Sec17/αSNAP, and Sec18/NSF. The energy for fusion (Step 5) derives from multiple sources: the completion of SNARE zippering, the binding energies which create the Sec17 structure surrounding the SNAREs, and the energy of bilayer distortion through Sec17 apolar loop insertion. *Cis*-SNARE complexes (Figure 7F) formed by fusion (Söllner *et al.*, 1993; Mayer *et al.*, 1996) are disassembled by Sec17, Sec18, and ATP (Step 6), freeing SNAREs from each other (Figure 7A) for later assembly in *trans*. Each of these components – the four SNAREs, the Rab Ypt7, HOPS, Sec17, and Sec18 – is part of this ordered pathway of associations and disassembly, constituting a holoenzyme for vacuole membrane fusion.

Our current studies reveal a general capacity of Sec17/αSNAP and Sec18/NSF to support fusion, even when little or no energy would be derived from completion of zippering. Sec17 provides a cage-like environment (Chakraborty *et al.*, 2010), albeit with side fenestrations (Schwartz *et al.*, 2017), which may favor SNARE zippering or, where zippering is blocked, allow the remaining SNARE domains to attain positions and conformations that approximate zippering. The apolar N-domains of the four Sec17s are clearly essential for fusion (Figure 5 and Figure 5—figure supplement 2), whether through positioning the Sec17s, facilitating their assembly, or directly inserting as a ‘membrane wedge’ and thereby contributing to bilayer disruption at the fusion site. The continued need for this apolar loop when Sec17 is integrally membrane-anchored (Figure 5—figure supplement 2) shows that it does not simply contribute to Sec17 membrane association. Elements of ‘Sec17 cage’ and ‘membrane wedge’ action are not mutually exclusive. Further work will be needed to determine the relative energies of Sec17 and Sec18 binding to the assembling 4-SNARE *trans*-complex, each of the four Sec17s inserting its apolar loops into the membrane, Sec17 forming lateral associations with other Sec17 molecules in the cage around the SNAREs, and complete SNARE zippering, as each of these helps to achieve the bilayer distortions of fusion.

Our current studies further our understanding of how Sec17(αSNAP), Sec18 (NSF), and SNAREs cooperate to promote membrane fusion. Sec17 has multiple functions: (a) It supports Sec18 association with SNARE complexes for their ATP-driven disassembly for subsequent rounds of fusion (Ungermann *et al.*, 1998; Choi *et al.*, 2018). Sec17/αSNAP and Sec18/NSF are also part of a quality control system that, for vacuoles, includes HOPS (Starai *et al.*, 2008) and, in the neuronal system, includes Munc18 and Munc13 (Ma *et al.*, 2013; Lai *et al.*, 2017). These disassembly reactions require ATP hydrolysis and can be interrupted by the Sec17 LALA mutation. (b) Sec17 promotes a conformational change that leads to complete SNARE zippering. While neuronal SNAREs, which are properly assembled (i.e., involving the Munc18/Munc13 pathway), will fully zipper with a high energy yield, this may not be true for all non-neuronal SNAREs. (c) Sec17 promotes fusion even when SNARE zippering is incomplete. Sec17 uses the partially zippered SNAREs as a platform to bind to the fusion site and its apolar N-domain loop to trigger fusion. Sec18 also has multiple functions: (a) Sec18/NSF drives ATP-driven SNARE disassembly (Zhao *et al.*, 2015), blocked by the Sec17 LALA

mutation. (b) Sec18 supports Sec17 for direct promotion of fusion, built on a platform of partially zippered SNAREs. Note that the loading of SNARE N-terminal residues into the pore of the D1 ring of NSF does not require hydrolysis (White *et al.*, 2018), so initial assembly of the NSF/ α SNAP/SNARE complex occurs in the absence of hydrolysis. This does not need ATP hydrolysis and is insensitive to the LALA mutation. Thirdly, SNAREs also have multiple functions: (a) They can completely zipper, thereby stressing the bilayer and triggering fusion (Weber *et al.*, 1998; Sutton *et al.*, 1998). As previously reported (Mima *et al.*, 2008; Song *et al.*, 2017), HOPS alone, without Sec17 or Sec18, will support slow SNARE-dependent fusion. (b) SNAREs support the assembly of a microdomain in which multiple fusion proteins and lipids become highly enriched (Fratti *et al.*, 2004). (c) As shown here, SNAREs form an essential platform for Sec17 and Sec18 to contribute to fusion independently of completion of zippering. With physiological levels of wild-type vacuolar SNAREs, rapid fusion requires Rab-activated HOPS, Sec17, Sec18, and ATP.

While intracellular fusion reactions share many requirements, such as for SNAREs and SM protein, there are major differences as well. Synaptic vesicle fusion and other calcium-dependent secretion systems require calcium, synaptotagmin, Munc13, and complexin, none of which have their obvious counterparts in calcium-independent systems. Vacuole and endosome fusion have their SM protein as an integral subunit of the tethering complex, which is not seen in other organelles. The similarities and differences in fusion pathways at each organelle will be clarified as each is more thoroughly studied.

Materials and methods

Key resources table

Reagent type (species) or resource	Designation	Source or reference	Identifiers	Additional information
Gene (<i>Saccharomyces cerevisiae</i>)	Nyv1	<i>Saccharomyces</i> Genome Database	SGD:S000004083	
Gene (<i>Saccharomyces cerevisiae</i>)	Vam3	<i>Saccharomyces</i> Genome Database	SGD:S000005632	
Gene (<i>Saccharomyces cerevisiae</i>)	Vti1	<i>Saccharomyces</i> Genome Database	SGD:S000004810	
Gene (<i>Saccharomyces cerevisiae</i>)	Vam7	<i>Saccharomyces</i> Genome Database	SGD:S000003180	
Gene (<i>Saccharomyces cerevisiae</i>)	Ypt7	<i>Saccharomyces</i> Genome Database	SGD:S000004460	
Gene (<i>Saccharomyces cerevisiae</i>)	Sec17	<i>Saccharomyces</i> Genome Database	SGD:S000000146	
Gene (<i>Saccharomyces cerevisiae</i>)	Sec18	<i>Saccharomyces</i> Genome Database	SGD:S000000284	
Gene (<i>Saccharomyces cerevisiae</i>)	Vps33	<i>Saccharomyces</i> Genome Database	SGD:S000004388	
Gene (<i>Saccharomyces cerevisiae</i>)	Vps39	<i>Saccharomyces</i> Genome Database	SGD:S000002235	
Gene (<i>Saccharomyces cerevisiae</i>)	Vps41	<i>Saccharomyces</i> Genome Database	SGD:S000002487	

Continued on next page

Continued

Reagent type (species) or resource	Designation	Source or reference	Identifiers	Additional information
Gene (<i>Saccharomyces cerevisiae</i>)	Vps16	<i>Saccharomyces</i> Genome Database	SGD:S000005966	
Gene (<i>Saccharomyces cerevisiae</i>)	Vps11	<i>Saccharomyces</i> Genome Database	SGD:S000004844	
Gene (<i>Saccharomyces cerevisiae</i>)	Vps18	<i>Saccharomyces</i> Genome Database	SGD:S000004138	
Peptide, recombinant protein	GST-R (Nyv1)	PMID: 18650938		Purified from <i>E. coli</i> .
Peptide, recombinant protein	GST-Qa (Vam3)	PMID: 18650938		Purified from <i>E. coli</i> .
Peptide, recombinant protein	GST-Qb (Vti1)	PMID: 18650938		Purified from <i>E. coli</i> .
Peptide, recombinant protein	His-R (Nyv1)	PMID: 22174414		Purified from <i>E. coli</i> .
Peptide, recombinant protein	GST-sQa (soluble)	PMID: 28637767		Purified from <i>E. coli</i> .
Peptide, recombinant protein	MBP-sQb (soluble)	PMID: 24088569		Purified from <i>E. coli</i> .
Peptide, recombinant protein	GST-Qb (Vti1) Δ	This study		Purified from <i>E. coli</i> .
Peptide, recombinant protein	GST-Qa (Vam3) Δ	This study		Purified from <i>E. coli</i> .
Peptide, recombinant protein	Qc (Vam7)	PMID: 17699614		Purified from <i>E. coli</i> .
Peptide, recombinant protein	Qc (Vam7)-tm	PMID: 23071309		Purified from <i>E. coli</i> .
Peptide, recombinant protein	Qc (Vam7) C208S, M250C	This study		Purified from <i>E. coli</i> .
Peptide, recombinant protein	Qc (Vam7) C208S, A316C	This study		Purified from <i>E. coli</i> .
Peptide, recombinant protein	MBP-Cys-sQb (SNARE domain)	PMID: 28637767		Purified from <i>E. coli</i> .
Peptide, recombinant protein	MBP-Cys-sQb (SNARE domain)	PMID: 28637767		Purified from <i>E. coli</i> .
Peptide, recombinant protein	Ypt7	PMID: 24088569		Purified from <i>E. coli</i> .

Continued on next page

Continued

Reagent type (species) or resource	Designation	Source or reference	Identifiers	Additional information
Peptide, recombinant protein	Ypt7-TM	PMID:31235584		Purified from <i>E. coli</i> .
Peptide, recombinant protein	Sec17	PMID:19414611		Purified from <i>E. coli</i> .
Peptide, recombinant protein	Sec17 FSMS	PMID:28925353		Purified from <i>E. coli</i> .
Peptide, recombinant protein	Sec17 KEKE	PMID:28925353		Purified from <i>E. coli</i> .
Peptide, recombinant protein	Sec17 LALA	PMID:19414611		Purified from <i>E. coli</i> .
Peptide, recombinant protein	GST-Sec17 6AtoN	This study		Purified from <i>E. coli</i> .
Peptide, recombinant protein	GST-Sec17-TM	PMID:28718762		Purified from <i>E. coli</i> .
Peptide, recombinant protein	GST-Sec17-TM FSMS	PMID:28718762		Purified from <i>E. coli</i> .
Peptide, recombinant protein	TEV protease	PMID:18007597		Purified from <i>E. coli</i> .
Peptide, recombinant protein	HOPS	PMID:18385512		Purified from <i>Saccharomyces cerevisiae</i> .
Antibody	Anti-Vam3 (rabbit polyclonal)	PMID:12566429	Wickner lab stock	WB: 1:2000
Antibody	Anti-Nyv1 (rabbit polyclonal)	PMID:10385523	Wickner lab stock	WB: 0.65 µg/ml
Antibody	Anti-Vti1 (rabbit polyclonal)	PMID:18007597	Wickner lab stock	WB: 0.47 µg/ml
Antibody	Anti-Vam7 (rabbit polyclonal)	PMID:14734531	Wickner lab stock	WB: 0.1 µg/ml
Antibody	Anti-Vps16 (rabbit polyclonal)	PMID:18007597	Wickner lab stock	WB: 1 µg/ml
Antibody	Anti-Vps33 (rabbit polyclonal)	PMID:10944212	Wickner lab stock	Inhibition assay: 1 µg
Antibody	Anti-Sec18 (rabbit polyclonal)	PMID:11483507	Wickner lab stock	Inhibition assay: 1 µg
Chemical compound, drug	Cy5-derivatized streptavidin	SeraCare Life Sciences	5270-0023	
Chemical compound, drug	Biotinylated PhycoE	Thermo Fisher Scientific	p811	
Chemical compound, drug	Streptavidin	Thermo Fisher Scientific	434302	
Chemical compound, drug	1,2-dilinoleoyl-sn-glycero-3-phosphocholine	Avanti polar lipids	850385	
Chemical compound, drug	1,2-dilinoleoyl-sn-glycero-3-phospho-L-serine	Avanti polar lipids	840040	
Chemical compound, drug	1,2-dilinoleoyl-sn-glycero-3-phosphoethanolamine	Avanti polar lipids	850755	
Chemical compound, drug	1,2-dilinoleoyl-sn-glycero-3-phosphate	Avanti polar lipids	840885	
Chemical compound, drug	L- α -phosphatidylinositol	Avanti polar lipids	840044	

Continued on next page

Continued

Reagent type (species) or resource	Designation	Source or reference	Identifiers	Additional information
Chemical compound, drug	1,2-dipalmitoyl-sn-glycerol	Avanti polar lipids	800816	
Chemical compound, drug	Ergosterol	Sigma	45480	
Chemical compound, drug	PI(3)P	Echelon Bioscience	P-3016	
Chemical compound, drug	Rhodamine DHPE	Invitrogen	L1392	
Chemical compound, drug	NBD-PE	Invitrogen	N360	
Chemical compound, drug	Marina-blue	Invitrogen	M12652	
Software and algorithms	UN-SCAN-IT	Silk Scientific		
Chemical compound, drug	Alexa Fluor 568 C5-maleimide	Thermo Fisher Scientific	A20341	
Chemical compound, drug	Oregon Green 488 Maleimide	Thermo Fisher Scientific	O6034	
Chemical compound, drug	Oregon Green 488 Maleimide	Thermo Fisher Scientific	O6034	
Chemical compound, drug	Pierce TCEP-HCl	Thermo Fisher Scientific	20490	
Chemical compound, drug	L-cysteine	Sigma-Aldrich	30089	

PI3P was from Echelon (Salt Lake City, Utah), ergosterol from Sigma (St. Louis, MO), fluorescent lipids from Thermo Fisher (Waltham, MA), and other lipids were from Avanti (Alabaster, AL). Bio-beads SM2 were from BioRad, Cy5-Streptavidin from SeraCare (Milford, MA), biotinylated phycoerythrin from Invitrogen (Eugene, OR), and underivatized streptavidin from Thermo Fisher. Spectrapor six dialysis tubing (7.5 mm diameter, 25 kDa cutoff) was from Spectrum Labs (Las Vegas, NV). Octyl- β -D-glucopyranoside was purchased from Anatrace (Maumee, OH).

Mutant constructions

Sec17 with six acidic amino acids mutated to neutral residues, GST-Sec17 (E34S, E35S, D38S, E73A, D74A, E75A), was generated by PCR with Phusion high-fidelity DNA polymerase (NEB). The DNA fragment was cloned into BamHI- and Sall-digested pGST parallel1 vector (*Sheffield et al., 1999*) with an In-Fusion kit (Takara Bio USA, Mountain View, CA). Using inverse PCR, pParallel1-GST-Sec17 mutant (E34S, E35S, and D38S) was amplified with Phusion high-fidelity DNA polymerase (NEB) from a GST-Sec17 construct. The amplified linear DNA was re-circularized with an In-fusion kit (Takara Bio USA). To generate Sec17 acidic to neutral mutants, pParallel1-GST-Sec17 mutant (E34S, E35S, and D38S) was amplified with a Sec17 E73A, D74A, and E75A mutant primer set using Phusion high-fidelity DNA polymerase (NEB) and re-circularized with an In-fusion kit (Takara Bio USA).

For Sec17-E34S, E35S, D38S,
 F: TCGTCGGCTGCTTCTCTTTGTGTCCAAGCAGCCAC
 R: AGAAGCAGCCGACGAAAACCTGTATGAATCAGAAC
 For Sec17 E73A, D74A, E75A,
 F: GGTAATGCAGCCGAGCAGGAAATACCTACGTAGA
 R: TGCGGCTGCATTACCAGCCTTTTCTGATAGTCAG

GST-sQa3 Δ with amino acyl residues 1–235 and GST-sQb3 Δ with amino acyl residues 1–160 were generated by PCR with Phusion high-fidelity DNA polymerase (NEB). DNA fragments were cloned into BamHI- and Sall-digested pGST parallel1 vector (*Sheffield et al., 1999*) with an In-Fusion kit (Takara Bio USA).

For GST-sQa3 Δ ,
 F: AGGGCGCCATGGATCCGATGTCCTTTTTCGACATCGA
 R: AGTTGAGCTCGTCGACTAGATATTCTCGTCTATGGTGG
 For GST-sQb3 Δ ,
 F: AGGGCGCCATGGATCCGATGAGTTCCTATTAATA
 R: AGTTGAGCTCGTCGACTACAAGGTCTGTCTTGCAATTT

To generate Qa with L238, M242, A245, L249, and A252 changed to Ala, Ser, or Gly, the pParallel1 GST vector with Qa lacking residues 228–257 was generated by inverse PCR with pParallel1 GST-Qa (*Mima et al., 2008*) using Phusion high-fidelity DNA polymerase (NEB). The DNA duplex with mutations (Gly, Ser, or Ala) of the +4 to +8 heptad repeats was cloned into the amplified vector bearing Qa 1–227 with an In-fusion kit (Takara Bio USA, Mountain View, CA).

For inverse PCR of pParallel1 GST and Qa 1–227,

F: GACCAGCATCAGAGGGACCG
 R: GTCTATGGTGGTTACTTGTT

For the Gly mutant of Qa,

Sequence 1: GTAACCACCATAGACGAGAATATCTCGCATGGCCATGATAACGGCCAGAA
 TGGCAACAAACAAGGCACCAGAGGGCGACCAGCATCAGAGG
 Sequence 2: CCTCTGATGCTGGTTCGCTTCTGGTGCCTTGTGTTGTTGCCATTCTGGCCGTTA
 TCATGGCCATGCGAGATATTCTCGTCTATGGTGGTTAC

For the Ser mutant of Qa,

Sequence 1: GTAACCACCATAGACGAGAATATCTCGCATAGCCATGATAACAGCCAGAA
 TAGCAACAAACAAGCACCAGAAGCGACCAGCATCAGAGG
 Sequence 2: CCTCTGATGCTGGTTCGCTTCTGGTGCCTTGTGTTGTTGCTATTCTGGCTGTTATCA
 TGGCTATGCGAGATATTCTCGTCTATGGTGGTTAC

For the Ala mutant of Qa,

Sequence 1: GTAACCACCATAGACGAGAATATCTCGCATGCCATGATAACGCCAGAA
 TGCCAACAAACAAGCCACCAGAGCCGACCAGCATCAGAGG
 Sequence 2: CCTCTGATGCTGGTTCGCTTCTGGTGGCTTGTGTTGTTGCCATTCTGGGCGTTA
 TCATGGGCATGCGAGATATTCTCGTCTATGGTGGTTAC

Vam7 mutants with cysteines inserted at the N- and C-termini of the SNARE domain were generated by inverse PCR with the Vam7 intein vector (*Schwartz and Merz, 2009*) and Phusion high-fidelity DNA polymerase (NEB). First, the native cysteine was removed by mutating it to serine (C208S) using the mutant primer set below. Vam7 mutants with cysteines inserted near the N- and C-termini of the SNARE domain, M250C and A316C, respectively, were generated from the cysteine-lacking plasmid in the same fashion.

For Vam7-C208S,
 F: GAAAGCGATGACATTGGTACAGCAAACATAGCTCA
 R: CAATGTCATCGCTTTCCTTGAGCAAGGACCTCAAT
 For Vam7-C208S,M250C (Qc with N-terminal cysteine),
 F: GGGCAGTGTCAAATGGTGC GCGATCAAGAACAA
 R: CCATTTGACTGCCCCCTGTTGCAAATCGTTAT
 For Vam7-C208S,A316C (Qc with C-terminal cysteine),
 F: CAACAGTTGTTGAATTCTCGAGCACCA
 R: CAACAACACTGTTGTTAAAATGTCTAGCCTTCTTGTGGC

Protein isolation

HOPS and prenyl-Ypt7 (Zick and Wickner, 2013), Ypt7-TM (Song et al., 2020), Sec17 (Schwartz and Merz, 2009), TM-anchored Sec17 and TM-anchored Sec17-F21SM22S (Song et al., 2017), Sec18 (Mayer et al., 1996), wild-type vacuolar SNAREs and his6-R (Mima et al., 2008; Schwartz and Merz, 2009; Zucchi and Zick, 2011; Izawa et al., 2012), sQb (Zick and Wickner, 2013) Qc-C208SM250C, Qc-C208SA316C, and Qc3Δ (Schwartz and Merz, 2009) were purified as described. sQa, sQa3Δ, and sQb3Δ were purified by a modification of prior methods (Zick and Wickner, 2013; Song et al., 2020). pGST-Parallel1 with sQa, sQa3Δ, or sQb3Δ was transformed into Rosetta2 (DE3)-pLysS cells (EMD Millipore, Billerica, MA). Luria–Bertani (LB) broth (100 ml) containing 100 μg/ml ampicillin and 34 μg/ml chloramphenicol was inoculated with a single colony. After overnight incubation with shaking at 37°C, 40 ml portions of the preculture were added to two 6 l flasks, each with 3 l of LB medium, containing 100 μg/ml ampicillin and 34 μg/ml chloramphenicol and shaken (200 rpm) at 37°C to an OD600 of 0.8. Isopropyl β-D-1-thiogalactopyranoside was added to 0.5 mM. After 3 hr of continued shaking at 37°C, bacteria were harvested by centrifugation (5000 rpm, 5 min, 4°C). Cell pellets were resuspended in 60 ml of 20 mM HEPES-NaOH (pH 7.4), 200 mM NaCl, 1 mM EDTA, 1 mM dithiothreitol (DTT), 200 mM phenylmethyl sulfonylfluoride, and 1 X protease inhibitor cocktail (Xu and Wickner, 1996). Resuspended cells were passed twice through a French press at 900 psi. The cell lysate was centrifuged (4°C, 1 hr, 50,000 rpm, SW 60Ti rotor [Beckman Coulter, Brea, CA]). The supernatant was added to 20 ml of Glutathione Agarose 4B resin (Genesee Scientific, San Diego, CA), which had been equilibrated with wash buffer (20 mM HEPES-NaOH (pH 7.4), 200 mM NaCl, and 1 mM EDTA, 1 mM DTT) and nutated at 4°C for 2 hr. The suspended resin was poured into a 2.5-cm-diameter column, drained, and washed with 100 ml wash buffer. The GST-tagged protein was eluted with 20 mM HEPES-NaOH (pH 7.4), 200 mM NaCl, 1 mM EDTA, 1 mM DTT, 5% glycerol, and 20 mM glutathione, and the GST tag removed by TEV protease.

Proteoliposome fusion

Proteoliposomes were prepared by detergent dialysis from β-octylglucoside-mixed micelles for fusion assays (Song et al., 2017; Song and Wickner, 2019) and SNARE assembly assays (Torng et al., 2020) as described. Briefly, for the fusion assay, proteoliposomes (1 mM lipid) were prepared with membrane-bound Ypt7 and R at 1:8000 and 1:16,000 molar ratios to lipid, respectively, and with luminal biotin-phycoerythrin. Proteoliposomes were also prepared with membrane-bound Ypt7 and the indicated Q-SNAREs at 1:8000 and 1:16,000 molar ratios to lipid, respectively, plus luminal Cy5-streptavidin. These were incubated separately for 10 min at 27°C with 1 μM GTP and 1 mM EDTA, and then MgCl₂ was added to 2 mM. After prewarming (27°C for 10 min) the separately GTP-exchanged proteoliposomes in a 384-well plate, fusion reactions were initiated by mixing 5 μl of each proteoliposome preparation and supplementing with other fusion factors in volumes summing to 10 μl, continuing incubation at 27°C in a Spectramax fluorescent plate reader. Fusion incubations (20 μl) in RB150 (20 mM HEPES/NaOH, pH 7.4, 150 mM NaCl, 10% glycerol) had proteoliposomes (0.5 mM total lipid concentration), 50 nM HOPS, the indicated concentrations of sSNAREs, 400 or 600 nM Sec17, 300 nM Sec18, 1 mM ATP or its analogs, and 3 mM MgCl₂, as modified in each figure legend.

SNARE assembly assay

Assays were performed as described previously (Torng et al., 2020) with one addendum. In brief, reactions (20 μl) were performed at 27°C in a SpectraMax Gemini XPS (Molecular Devices) plate reader. Standard reactions include HOPS (160 nM), proteoliposomes (0.5 mM lipid, with SNARE and Ypt7 at a molar ratio of either 1:2000 or 1:4000 for Ypt7/R proteoliposomes and Ypt7/RQa proteoliposomes, respectively), and fluorescently labeled Qb and Qc (1 μM), and sQa (1 μM) as necessary. These were incubated for 60 min, and then Sec17 was added to 500 nM. Three fluorescence channels were read simultaneously at intervals of 30 s: the donor channel Oregon Green 488 from Qc (excitation [ex]: 497 nm; emission [em]: 527 nm; cutoff [c/o]: 515 nm), the acceptor channel Alexa Fluor 568 from Qb (ex: 568 nm; em: 605 nm; c/o: 590 nm), and the FRET channel (ex: 490 nm; em: 615 nm; c/o: 590 nm). For each time point, the bleed through-corrected FRET signal was obtained by subtracting the background signals coming from the donor and acceptor channels from the signal in the FRET channel as detailed in Torng et al., 2020. This was further corrected by

dividing by the geometric mean of the donor and acceptor signals. The final corrected signal, reported as 'Average FRET efficiency,' is a combined measure of the proportion of fluorescent SNAREs undergoing FRET and their average FRET efficiency.

Molecular models

MODELLER (*Webb and Sali, 2016*) was used to create individual homology models of the vacuolar SNARE complex (Nyv1, Vam3, Vti1, Vam7), and of Sec18 starting from the coordinates of synaptobrevin-2, SNAP-25, syntaxin-1A, and NSF in the cryo-EM structure of the neuronal NSF/ α SNAP/SNARE complex (PDB ID 3J96) (*Zhao et al., 2015*). For Sec18, the linker between the N and D1 domains was deleted from the generated homology model since there was no information about these linkers in this structure (PDB ID 3J96) of the neuronal 20S complex.

The MODELLER protocol consisted of an alignment step (python script file align.py) and a modeling step (python script file modeler-input.py). The script files are shown here for synaptobrevin (nyv1):

align.py

```
from modeller import *
env = environ()
aln = alignment(env)
mdl = model(env, file='sb.pdb', model_segment=('FIRST:K','LAST:K'))
aln.append_model(mdl, align_codes='sbK', atom_files='sb.pdb')
aln.append(file='target_sequence.pir', align_codes='nyv1')
aln.salign(local_alignment = True, rr_file='${LIB}/blosum62.sim.mat',
gap_penalties_1d=(-600,-600),
output='',
align_block = 15, # no. of seqs. in first MSA
align_what='PROFILE',
alignment_type='PAIRWISE',
comparison_type='PSSM', # or 'MAT' (Caution: Method NOT benchmarked# for 'MAT')
similarity_flag = True, # The score matrix is not rescaled
substitution = True, # The BLOSUM62 substitution values are
# multiplied to the corr. coef.
#write_weights = True,
#output_weights_file='test.mtx', # optional, to write weight matrix
smooth_prof_weight = 10.0) # For mixing data with priors
aln.edit(edit_align_codes='nyv1', base_align_codes='rest',min_base_entries = 1,
overhang = 0)
aln.write(file='nyv1.ali', alignment_format='PIR')
aln.write(file='nyv1.pap', alignment_format='PAP')
```

modeler-input.py

```
from modeller import *
from modeller.automodel import *
env = environ()
a = automodel(env, alnfile='nyv1.ali', knowns='sbK', sequence='nyv1', assess_methods=
(assess.DOPE, assess.GA341))
a.very_fast()
a.starting_model = 1
a.ending_model = 1
a.make()
```

The homology models of Nyv1, Vam3, Vti1, Vam7, and Sec18, together with the crystal structure of Sec17 (PDB ID 1QQE) (*Rice and Brunger, 1999*), were fit into the cryo-EM structure of the neuronal NSF/ α SNAP/SNARE complex (PDB ID 3J96) (*Zhao et al., 2015*). The fit was performed by using the 'align' feature of PyMol to individually superimpose the coordinates of the vacuolar proteins with the corresponding coordinates of the neuronal proteins in the structure of the neuronal NSF/ α SNAP/SNARE complex.

Acknowledgements

We thank Gustav Lienhard, Charles Barlowe, Frederick Hughson, Michael Zick, Christian Ungermann, Jose Rizo, and Randy Schekman for insightful suggestions. This work was supported by grants R35GM118037 (to WW) and R37MH63105 (to ATB) from the NIH.

Additional information

Competing interests

Axel T Brunger: Reviewing editor, *eLife*. The other authors declare that no competing interests exist.

Funding

Funder	Grant reference number	Author
National Institutes of Health	R35GM118037	William T Wickner
National Institutes of Health	R37MH63105	Axel T Brunger

The funders had no role in study design, data collection and interpretation, or the decision to submit the work for publication.

Author contributions

Hongki Song, Conceptualization, Data curation, Software, Formal analysis, Validation, Investigation, Visualization, Methodology, Writing - review and editing; Thomas L Torng, Conceptualization, Data curation, Software, Formal analysis, Investigation, Visualization, Methodology, Writing - review and editing; Amy S Orr, Conceptualization, Data curation, Formal analysis, Investigation, Visualization, Methodology, Writing - review and editing; Axel T Brunger, Conceptualization, Resources, Data curation, Software, Formal analysis, Funding acquisition, Visualization, Project administration, Writing - review and editing; William T Wickner, Conceptualization, Resources, Supervision, Funding acquisition, Writing - original draft, Project administration, Writing - review and editing

Author ORCIDs

Hongki Song  <https://orcid.org/0000-0002-3761-5434>

Thomas L Torng  <http://orcid.org/0000-0003-2295-2777>

Amy S Orr  <https://orcid.org/0000-0002-0266-0390>

Axel T Brunger  <http://orcid.org/0000-0001-5121-2036>

William T Wickner  <https://orcid.org/0000-0001-8431-0468>

Decision letter and Author response

Decision letter <https://doi.org/10.7554/eLife.67578.sa1>

Author response <https://doi.org/10.7554/eLife.67578.sa2>

Additional files

Supplementary files

- Transparent reporting form

Data availability

All data generated or analyzed during this study are included in the manuscript and supporting files. Source data files have been provided for Figures 1, 2, 3 4, 5, and 6.

The following previously published datasets were used:

Author(s)	Year	Dataset title	Dataset URL	Database and Identifier
Zhao M, Wu S,	2015	Structure of 20S supercomplex	https://www.rcsb.org/	RCSB Protein Data

Cheng Y, Brunger AT		determined by single particle cryoelectron microscopy (State I)	structure/3j96	Bank, 3J96
Rice LM, Brunger AT	1999	CRYSTAL STRUCTURE OF THE VESICULAR TRANSPORT PROTEIN SEC17	https://www.rcsb.org/structure/1QQE	RCSB Protein Data Bank, 1QQE

References

- Aeffner S**, Reusch T, Weinhausen B, Salditt T. 2012. Energetics of stalk intermediates in membrane fusion are controlled by lipid composition. *PNAS* **109**:E1609–E1618. DOI: <https://doi.org/10.1073/pnas.1119442109>, PMID: 22589300
- Baker RW**, Jeffrey PD, Zick M, Phillips BP, Wickner WT, Hughson FM. 2015. A direct role for the Sec1/Munc18-family protein Vps33 as a template for SNARE assembly. *Science* **349**:1111–1114. DOI: <https://doi.org/10.1126/science.aac7906>, PMID: 26339030
- Barnard RJ**, Morgan A, Burgoyne RD. 1997. Stimulation of NSF ATPase activity by alpha-SNAP is required for SNARE complex disassembly and exocytosis. *Journal of Cell Biology* **139**:875–883. DOI: <https://doi.org/10.1083/jcb.139.4.875>, PMID: 9362506
- Brett CL**, Plemel RL, Lobingier BT, Lobinger BT, Vignali M, Fields S, Merz AJ. 2008. Efficient termination of vacuolar rab GTPase signaling requires coordinated action by a GAP and a protein kinase. *Journal of Cell Biology* **182**:1141–1151. DOI: <https://doi.org/10.1083/jcb.200801001>, PMID: 18809726
- Chakraborty K**, Chatila M, Sinha J, Shi Q, Poschner BC, Sikor M, Jiang G, Lamb DC, Hartl FU, Hayer-Hartl M. 2010. Chaperonin-catalyzed rescue of kinetically trapped states in protein folding. *Cell* **142**:112–122. DOI: <https://doi.org/10.1016/j.cell.2010.05.027>, PMID: 20603018
- Cheever ML**, Sato TK, de Beer T, Kutateladze TG, Emr SD, Overduin M. 2001. Phox domain interaction with PtdIns(3)P targets the Vam7 t-SNARE to vacuole membranes. *Nature Cell Biology* **3**:613–618. DOI: <https://doi.org/10.1038/35083000>, PMID: 11433291
- Choi UB**, Zhao M, White KI, Pfuetzner RA, Esquivies L, Zhou Q, Brunger AT. 2018. NSF-mediated disassembly of on- and off-pathway SNARE complexes and inhibition by complexin. *eLife* **7**:e36497. DOI: <https://doi.org/10.7554/eLife.36497>, PMID: 29985126
- Clary DO**, Griff IC, Rothman JE. 1990. SNAPs, a family of NSF attachment proteins involved in intracellular membrane fusion in animals and yeast. *Cell* **61**:709–721. DOI: [https://doi.org/10.1016/0092-8674\(90\)90482-T](https://doi.org/10.1016/0092-8674(90)90482-T)
- Collins KM**, Thorngren NL, Fratti RA, Wickner WT. 2005. Sec17p and HOPS, in distinct SNARE complexes, mediate SNARE complex disruption or assembly for fusion. *The EMBO Journal* **24**:1775–1786. DOI: <https://doi.org/10.1038/sj.emboj.7600658>, PMID: 15889152
- Fasshauer D**, Bruns D, Shen B, Jahn R, Brünger AT. 1997. A structural change occurs upon binding of syntaxin to SNAP-25. *Journal of Biological Chemistry* **272**:4582–4590. DOI: <https://doi.org/10.1074/jbc.272.7.4582>, PMID: 9020186
- Fasshauer D**, Sutton RB, Brunger AT, Jahn R. 1998. Conserved structural features of the synaptic fusion complex: snare proteins reclassified as Q- and R-SNAREs. *PNAS* **95**:15781–15786. DOI: <https://doi.org/10.1073/pnas.95.26.15781>, PMID: 9861047
- Fiebig KM**, Rice LM, Pollock E, Brunger AT. 1999. Folding intermediates of SNARE complex assembly. *Nature Structural Biology* **6**:117–123. DOI: <https://doi.org/10.1038/5803>, PMID: 10048921
- Fratti RA**, Jun Y, Merz AJ, Margolis N, Wickner W. 2004. Interdependent assembly of specific regulatory lipids and membrane fusion proteins into the vertex ring domain of docked vacuoles. *Journal of Cell Biology* **167**:1087–1098. DOI: <https://doi.org/10.1083/jcb.200409068>, PMID: 15611334
- Fukuda R**, McNew JA, Weber T, Parlati F, Engel T, Nickel W, Rothman JE, Söllner TH. 2000. Functional architecture of an intracellular membrane t-SNARE. *Nature* **407**:198–202. DOI: <https://doi.org/10.1038/35025084>, PMID: 11001059
- Gao Y**, Zorman S, Gundersen G, Xi Z, Ma L, Sirinakakis G, Rothman JE, Zhang Y. 2012. Single reconstituted neuronal SNARE complexes zipper in three distinct stages. *Science* **337**:1340–1343. DOI: <https://doi.org/10.1126/science.1224492>, PMID: 22903523
- Haas A**, Wickner W. 1996. Homotypic vacuole fusion requires Sec17p (yeast alpha-SNAP) and Sec18p (yeast NSF). *The EMBO Journal* **15**:3296–3305. DOI: <https://doi.org/10.1002/j.1460-2075.1996.tb00694.x>, PMID: 8670830
- Hazzard J**, Südhof TC, Rizo J. 1999. NMR analysis of the structure of synaptobrevin and of its interaction with syntaxin. *Journal of Biomolecular NMR* **14**:203–207. DOI: <https://doi.org/10.1023/a:1008382027065>, PMID: 10481273
- Hickey CM**, Wickner W. 2010. HOPS initiates vacuole docking by tethering membranes before trans-SNARE complex assembly. *Molecular Biology of the Cell* **21**:2297–2305. DOI: <https://doi.org/10.1091/mbc.e10-01-0044>, PMID: 20462954
- Ho B**, Baryshnikova A, Brown GW. 2018. Unification of protein abundance datasets yields a quantitative *Saccharomyces cerevisiae* proteome. *Cell Systems* **6**:192–205. DOI: <https://doi.org/10.1016/j.cels.2017.12.004>, PMID: 29361465
- Izawa R**, Onoue T, Furukawa N, Mima J. 2012. Distinct contributions of vacuolar qabc- and R-SNARE proteins to membrane fusion specificity. *Journal of Biological Chemistry* **287**:3445–3453. DOI: <https://doi.org/10.1074/jbc.M111.307439>, PMID: 22174414

- Jiao J, He M, Port SA, Baker RW, Xu Y, Qu H, Xiong Y, Wang Y, Jin H, Eisemann TJ, Hughson FM, Zhang Y. 2018. Munc18-1 catalyzes neuronal SNARE assembly by templating SNARE association. *eLife* **7**:e41771. DOI: <https://doi.org/10.7554/eLife.41771>, PMID: 30540253
- Jun Y, Wickner W. 2019. Sec17 (α -SNAP) and Sec18 (NSF) restrict membrane fusion to R-SNAREs, Q-SNAREs, and SM proteins from identical compartments. *PNAS* **116**:23573–23581. DOI: <https://doi.org/10.1073/pnas.1913985116>, PMID: 31685636
- Lai Y, Choi UB, Leitz J, Rhee HJ, Lee C, Altas B, Zhao M, Pfuetzner RA, Wang AL, Brose N, Rhee J, Brunger AT. 2017. Molecular mechanisms of synaptic vesicle priming by Munc13 and Munc18. *Neuron* **95**:591–607. DOI: <https://doi.org/10.1016/j.neuron.2017.07.004>, PMID: 28772123
- Ma C, Li W, Xu Y, Rizo J. 2011. Munc13 mediates the transition from the closed syntaxin-Munc18 complex to the SNARE complex. *Nature Structural & Molecular Biology* **18**:542–549. DOI: <https://doi.org/10.1038/nsmb.2047>, PMID: 21499244
- Ma C, Su L, Seven AB, Xu Y, Rizo J. 2013. Reconstitution of the vital functions of Munc18 and Munc13 in neurotransmitter release. *Science* **339**:421–425. DOI: <https://doi.org/10.1126/science.1230473>
- Ma L, Kang Y, Jiao J, Rebane AA, Cha HK, Xi Z, Qu H, Zhang Y. 2016. α -SNAP enhances SNARE zippering by stabilizing the SNARE Four-Helix bundle. *Cell Reports* **15**:531–539. DOI: <https://doi.org/10.1016/j.celrep.2016.03.050>, PMID: 27068468
- Marz KE, Lauer JM, Hanson PI. 2003. Defining the SNARE complex binding surface of alpha-SNAP: implications for SNARE complex disassembly. *The Journal of Biological Chemistry* **278**:27000–27008. DOI: <https://doi.org/10.1074/jbc.M302003200>, PMID: 12730228
- Mayer A, Wickner W, Haas A. 1996. Sec18p (NSF)-driven release of Sec17p (alpha-SNAP) can precede docking and fusion of yeast vacuoles. *Cell* **85**:83–94. DOI: [https://doi.org/10.1016/S0092-8674\(00\)81084-3](https://doi.org/10.1016/S0092-8674(00)81084-3), PMID: 8620540
- Mima J, Hickey CM, Xu H, Jun Y, Wickner W. 2008. Reconstituted membrane fusion requires regulatory lipids, SNAREs and synergistic SNARE chaperones. *The EMBO Journal* **27**:2031–2042. DOI: <https://doi.org/10.1038/emboj.2008.139>, PMID: 18650938
- Min D, Kim K, Hyeon C, Hoon Cho Y, Shin Y-K, Yoon T-Y. 2013. Mechanical unzipping and re-zipping of a single SNARE complex reveals hysteresis as a force-generating mechanism. *Nature Communications* **4**:ncomms2692. DOI: <https://doi.org/10.1038/ncomms2692>
- Nichols BJ, Ungermann C, Pelham HR, Wickner WT, Haas A. 1997. Homotypic vacuolar fusion mediated by t- and v-SNAREs. *Nature* **387**:199–202. DOI: <https://doi.org/10.1038/387199a0>, PMID: 9144293
- Ohya T, Miaczynska M, Coskun U, Lommer B, Runge A, Drechsel D, Kalaidzidis Y, Zerial M. 2009. Reconstitution of rab- and SNARE-dependent membrane fusion by synthetic endosomes. *Nature* **459**:1091–1097. DOI: <https://doi.org/10.1038/nature08107>, PMID: 19458617
- Orr A, Wickner W, Rusin SF, Kettenbach AN, Zick M. 2015. Yeast vacuolar HOPS, regulated by its kinase, exploits affinities for acidic lipids and rab:gtp for membrane binding and to catalyze tethering and fusion. *Molecular Biology of the Cell* **26**:305–315. DOI: <https://doi.org/10.1091/mbc.E14-08-1298>, PMID: 25411340
- Orr A, Song H, Rusin SF, Kettenbach AN, Wickner W. 2017. HOPS catalyzes the interdependent assembly of each vacuolar SNARE into a SNARE complex. *Molecular Biology of the Cell* **28**:975–983. DOI: <https://doi.org/10.1091/mbc.e16-10-0743>, PMID: 28148647
- Pace CN, Scholtz JM. 1998. A Helix propensity scale based on experimental studies of peptides and proteins. *Biophysical Journal* **75**:422–427. DOI: [https://doi.org/10.1016/S0006-3495\(98\)77529-0](https://doi.org/10.1016/S0006-3495(98)77529-0), PMID: 9649402
- Rice LM, Brunger AT. 1999. Crystal structure of the vesicular transport protein Sec17. *Molecular Cell* **4**:85–95. DOI: [https://doi.org/10.1016/S1097-2765\(00\)80190-2](https://doi.org/10.1016/S1097-2765(00)80190-2)
- Richmond JE, Weimer RM, Jorgensen EM. 2001. An open form of syntaxin bypasses the requirement for UNC-13 in vesicle priming. *Nature* **412**:338–341. DOI: <https://doi.org/10.1038/35085583>, PMID: 11460165
- Ryu JK, Min D, Rah SH, Kim SJ, Park Y, Kim H, Hyeon C, Kim HM, Jahn R, Yoon TY. 2015. Spring-loaded unraveling of a single SNARE complex by NSF in one round of ATP turnover. *Science* **347**:1485–1489. DOI: <https://doi.org/10.1126/science.aaa5267>, PMID: 25814585
- Schwartz ML, Nickerson DP, Lobingier BT, Plemel RL, Duan M, Angers CG, Zick M, Merz AJ. 2017. Sec17 (α -SNAP) and an SM-tethering complex regulate the outcome of SNARE zippering in vitro and in vivo. *eLife* **6**:e27396. DOI: <https://doi.org/10.7554/eLife.27396>, PMID: 28925353
- Schwartz ML, Merz AJ. 2009. Capture and release of partially zipped trans-SNARE complexes on intact organelles. *Journal of Cell Biology* **185**:535–549. DOI: <https://doi.org/10.1083/jcb.200811082>, PMID: 19414611
- Seals DF, Eitzen G, Margolis N, Wickner WT, Price A. 2000. A ypt/Rab effector complex containing the Sec1 homolog Vps33p is required for homotypic vacuole fusion. *PNAS* **97**:9402–9407. DOI: <https://doi.org/10.1073/pnas.97.17.9402>, PMID: 10944212
- Sheffield P, Garrard S, Derewenda Z. 1999. Overcoming expression and purification problems of RhoGDI using a family of "parallel" expression vectors. *Protein Expression and Purification* **15**:34–39. DOI: <https://doi.org/10.1006/prep.1998.1003>, PMID: 10024467
- Söllner T, Bennett MK, Whiteheart SW, Scheller RH, Rothman JE. 1993. A protein assembly-disassembly pathway in vitro that may correspond to sequential steps of synaptic vesicle docking, activation, and fusion. *Cell* **75**:409–418. DOI: [https://doi.org/10.1016/0092-8674\(93\)90376-2](https://doi.org/10.1016/0092-8674(93)90376-2), PMID: 8221884
- Song H, Orr A, Duan M, Merz AJ, Wickner W. 2017. Sec17/Sec18 act twice, enhancing membrane fusion and then disassembling cis-SNARE complexes. *eLife* **6**:e26646. DOI: <https://doi.org/10.7554/eLife.26646>, PMID: 28718762

- Song H**, Orr AS, Lee M, Harner ME, Wickner WT. 2020. HOPS recognizes each SNARE, assembling ternary trans-complexes for rapid fusion upon engagement with the 4th SNARE. *eLife* **9**:e53559. DOI: <https://doi.org/10.7554/eLife.53559>, PMID: 31961324
- Song H**, Wickner W. 2017. A short region upstream of the yeast vacuolar Qa-SNARE heptad-repeats promotes membrane fusion through enhanced SNARE complex assembly. *Molecular Biology of the Cell* **28**:2282–2289. DOI: <https://doi.org/10.1091/mbc.e17-04-0218>, PMID: 28637767
- Song H**, Wickner W. 2019. Tethering guides fusion-competent trans-SNARE assembly. *PNAS* **116**:13952–13957. DOI: <https://doi.org/10.1073/pnas.1907640116>, PMID: 31235584
- Sørensen JB**, Wiederhold K, Müller EM, Milosevic I, Nagy G, de Groot BL, Grubmüller H, Fasshauer D. 2006. Sequential N- to C-terminal SNARE complex assembly drives priming and fusion of secretory vesicles. *The EMBO Journal* **25**:955–966. DOI: <https://doi.org/10.1038/sj.emboj.7601003>, PMID: 16498411
- Starai VJ**, Hickey CM, Wickner W. 2008. HOPS proofreads the trans-SNARE complex for yeast vacuole fusion. *Molecular Biology of the Cell* **19**:2500–2508. DOI: <https://doi.org/10.1091/mbc.e08-01-0077>, PMID: 18385512
- Stepien KP**, Rizo J. 2021. Synaptotagmin-1-, Munc18-1-, and Munc13-1-dependent liposome fusion with a few neuronal SNAREs. *PNAS* **118**:e2019314118. DOI: <https://doi.org/10.1073/pnas.2019314118>, PMID: 33468652
- Stroupe C**, Collins KM, Fratti RA, Wickner W. 2006. Purification of active HOPS complex reveals its affinities for phosphoinositides and the SNARE Vam7p. *The EMBO Journal* **25**:1579–1589. DOI: <https://doi.org/10.1038/sj.emboj.7601051>, PMID: 16601699
- Stroupe C**, Hickey CM, Mima J, Burfeind AS, Wickner W. 2009. Minimal membrane docking requirements revealed by reconstitution of rab GTPase-dependent membrane fusion from purified components. *PNAS* **106**:17626–17633. DOI: <https://doi.org/10.1073/pnas.0903801106>, PMID: 19826089
- Sutton RB**, Fasshauer D, Jahn R, Brunger AT. 1998. Crystal structure of a SNARE complex involved in synaptic exocytosis at 2.4 Å resolution. *Nature* **395**:347–353. DOI: <https://doi.org/10.1038/26412>, PMID: 9759724
- Torgg T**, Song H, Wickner W. 2020. Asymmetric rab activation of vacuolar HOPS to catalyze SNARE complex assembly. *Molecular Biology of the Cell* **31**:1060–1068. DOI: <https://doi.org/10.1091/mbc.E20-01-0019>, PMID: 32160129
- Ungermann C**, Nichols BJ, Pelham HR, Wickner W. 1998. A vacuolar v-t-SNARE complex, the predominant form in vivo and on isolated vacuoles, is disassembled and activated for docking and fusion. *Journal of Cell Biology* **140**:61–69. DOI: <https://doi.org/10.1083/jcb.140.1.61>, PMID: 9425154
- Wada Y**, Ohsumi Y, Anraku Y. 1992. Genes for directing vacuolar morphogenesis in *Saccharomyces cerevisiae*. I. Isolation and characterization of two classes of vam mutants. *Journal of Biological Chemistry* **267**:18665–18670. DOI: [https://doi.org/10.1016/S0021-9258\(19\)37012-7](https://doi.org/10.1016/S0021-9258(19)37012-7), PMID: 1526998
- Webb B**, Sali A. 2016. Comparative protein structure modeling using MODELLER. *Current Protocols in Bioinformatics* **54**:139–148. DOI: <https://doi.org/10.1002/cpbi.3>
- Weber T**, Zemelman BV, McNew JA, Westermann B, Gmachl M, Parlati F, Söllner TH, Rothman JE. 1998. SNAREpins: minimal machinery for membrane fusion. *Cell* **92**:759–772. DOI: [https://doi.org/10.1016/S0092-8674\(00\)81404-X](https://doi.org/10.1016/S0092-8674(00)81404-X), PMID: 9529252
- White KI**, Zhao M, Choi UB, Pfuetzner RA, Brunger AT. 2018. Structural principles of SNARE complex recognition by the AAA+ protein NSF. *eLife* **7**:e38888. DOI: <https://doi.org/10.7554/eLife.38888>, PMID: 30198481
- Wickner W**. 2010. Membrane fusion: five lipids, four SNAREs, three chaperones, two nucleotides, and a rab, all dancing in a ring on yeast vacuoles. *Annual Review of Cell and Developmental Biology* **26**:115–136. DOI: <https://doi.org/10.1146/annurev-cellbio-100109-104131>
- Winter U**, Chen X, Fasshauer D. 2009. A conserved membrane attachment site in alpha-SNAP facilitates N-ethylmaleimide-sensitive factor (NSF)-driven SNARE complex disassembly. *Journal of Biological Chemistry* **284**:31817–31826. DOI: <https://doi.org/10.1074/jbc.M109.045286>, PMID: 19762473
- Xu H**, Jun Y, Thompson J, Yates J, Wickner W. 2010. HOPS prevents the disassembly of trans-SNARE complexes by Sec17p/Sec18p during membrane fusion. *The EMBO Journal* **29**:1948–1960. DOI: <https://doi.org/10.1038/emboj.2010.97>, PMID: 20473271
- Xu Z**, Wickner W. 1996. Thioredoxin is required for vacuole inheritance in *Saccharomyces cerevisiae*. *Journal of Cell Biology* **132**:787–794. DOI: <https://doi.org/10.1083/jcb.132.5.787>, PMID: 8603912
- Zhang Y**. 2017. Energetics, kinetics, and pathway of SNARE folding and assembly revealed by optical tweezers. *Protein Science* **26**:1252–1265. DOI: <https://doi.org/10.1002/pro.3116>, PMID: 28097727
- Zhao M**, Wu S, Zhou Q, Vivona S, Cipriano DJ, Cheng Y, Brunger AT. 2015. Mechanistic insights into the recycling machine of the SNARE complex. *Nature* **518**:61–67. DOI: <https://doi.org/10.1038/nature14148>
- Zick M**, Orr A, Schwartz ML, Merz AJ, Wickner WT. 2015. Sec17 can trigger fusion of trans-SNARE paired membranes without Sec18. *PNAS* **112**:E2290–E2297. DOI: <https://doi.org/10.1073/pnas.1506409112>, PMID: 25902545
- Zick M**, Wickner W. 2013. The tethering complex HOPS catalyzes assembly of the soluble SNARE Vam7 into fusogenic trans-SNARE complexes. *Molecular Biology of the Cell* **24**:3746–3753. DOI: <https://doi.org/10.1091/mbc.e13-07-0419>, PMID: 24088569
- Zick M**, Wickner WT. 2014. A distinct tethering step is vital for vacuole membrane fusion. *eLife* **3**:e03251. DOI: <https://doi.org/10.7554/eLife.03251>, PMID: 25255215
- Zick M**, Wickner W. 2016. Improved reconstitution of yeast vacuole fusion with physiological SNARE concentrations reveals an asymmetric rab(GTP) requirement. *Molecular Biology of the Cell* **27**:2590–2597. DOI: <https://doi.org/10.1091/mbc.e16-04-0230>, PMID: 27385334

Zucchi PC, Zick M. 2011. Membrane fusion catalyzed by a rab, SNAREs, and SNARE chaperones is accompanied by enhanced permeability to small molecules and by lysis. *Molecular Biology of the Cell* **22**:4635–4646.
DOI: <https://doi.org/10.1091/mbc.e11-08-0680>, PMID: 21976702